

新疆东天山土屋斑岩铜矿床地球化学、年代学、Lu-Hf 同位素及其地质意义^{*}

王银宏¹ 薛春纪¹ 刘家军¹ 王建平¹ 杨俊弢² 张方方¹ 赵泽南¹ 赵云江²

WANG YinHong¹, XUE ChunJi¹, LIU JiaJun¹, WANG JianPing¹, YANG JunTao², ZHANG FangFang¹, ZHAO ZeNan¹ and ZHAO YunJiang²

1. 中国地质大学地质过程与矿产资源国家重点实验室 北京 100083

2. 新疆地质矿产开发局第一地质大队 昌吉 831100

1. State Key Laboratory of Geological Processes and Mineral Resources, China University of Geosciences, Beijing 100083, China

2. No. 1 Geological Party, Xinjiang Bureau of Geology and Mineral Exploration, Changji 831100, China

2014-02-10 收稿, 2014-06-07 改回.

Wang YH, Xue CJ, Liu JJ, Wang JP, Yang JT, Zhang FF, Zhao ZN and Zhao YJ. 2014. Geochemistry, geochronology, Hf isotope, and geological significance of the Tuwu porphyry copper deposit in eastern Tianshan, Xinjiang. *Acta Petrologica Sinica*, 30(11):3383–3399

Abstract The petrogenesis and geodynamic setting of magmatic rocks in eastern Tianshan are attracting increasing attention. This study explores these issues by providing SIMS zircon U-Pb dating, whole-rock geochemical, and Lu-Hf isotope data of the Tuwu porphyry copper deposit of eastern Tianshan, Xinjiang. The Tuwu porphyry copper deposit is located in the middle of the Late Paleozoic Dananhu-Tousuquan arc belt in the eastern Tianshan tectonic belt. The Carboniferous Qieshan Group is the main ore-hosting stratum. The andesite and dioritic porphyrite are the ore-hosting rocks, while the tonalitic rocks are the ore-bearing rocks. SIMS zircon U-Pb dating data indicate that the ore-bearing rocks occurred around 335Ma, and that mineralization of the Tuwu porphyry copper deposit occurred during the same period as that of the rock formation in the region or slightly later. The andesite and dioritic porphyrite are island arc volcanic rocks and formed by the same magmatism. However, the mineralized tonalitic rocks have adakitic characteristics. In situ Hf isotopic analyses of zircons yielded positive initial $\varepsilon_{\text{Hf}}(t)$ values ranging from +6.3 to +16.1, indicating the ore-bearing rocks were most likely derived from partial melting of a subducted oceanic slab. Therefore, we suppose that the North Tianshan oceanic crust subducted northward beneath the Dananhu-Tousuquan arc belt during the Early Carboniferous, and the Tuwu adakitic magmas were derived from partial melting of the subducted oceanic slab, hybridized subsequently by peridotite in the mantle wedge. During the adakitic magmas ascent, large amounts of metallogenic elements were released, and accumulated further on the top of the rock bodies.

Key words Tuwu porphyry copper deposit; SIMS zircon U-Pb dating; Geochemistry; Lu-Hf isotope; Eastern Tianshan

摘 要 新疆东天山地区岩浆岩的岩石成因和地球动力学背景备受关注。本文获得的东天山土屋斑岩铜矿床 SIMS 锆石 U-Pb 定年、全岩元素地球化学和 Lu-Hf 同位素数据, 以对这一问题进行约束。土屋斑岩铜矿床位于新疆东天山造山带晚古生代大南湖-头苏泉岛弧带中, 赋矿地层为下石炭统企鵝山群, 赋矿围岩主要为安山岩和闪长玢岩, 含矿岩石主要为英云闪长岩。本文 SIMS 锆石 U-Pb 定年结果表明, 土屋地区含矿岩体大约侵位于 335Ma, 土屋斑岩铜矿床成矿时代与成岩时代基本一致或稍晚。地球化学数据显示安山岩和闪长玢岩具有同源性及岛弧火山岩的特点, 英云闪长岩具有埃达克质岩石的特征。土屋英云闪长岩具不均一的锆石 $\varepsilon_{\text{Hf}}(t)$ 正值(+6.3 ~ +16.1), 表明其可能来源于俯冲板片的部分熔融。土屋斑岩铜矿床含矿岩体很可能是在早石炭世北天山洋板块北向俯冲的地球动力学背景下, 大洋板片发生部分熔融形成埃达克质岩浆, 在熔融过程中同时析出金属, 随埃达克质岩浆一起上升, 并与地幔橄榄岩发生交代作用, 在岩体顶部富集成矿。

^{*} 本文受中国地质调查局综合研究项目(1212011085471、1212011220923)、高等学校博士学科点专项科研基金(20130022110001)、高等学校学科创新引智计划(B07011)、国家自然科学基金项目(40973035)和中国地质大学(北京)基本科研业务费专项资金资助项目优秀导师基金联合资助。

第一作者简介: 王银宏, 男, 1973 年生, 博士, 副教授, 矿床学专业, E-mail: wyh@cugb.edu.cn

关键词 土屋斑岩铜矿床; SIMS 锆石 U-Pb 定年; 地球化学; Lu-Hf 同位素; 东天山
中图法分类号 P597.3; P618.41

作为中亚造山带晚古生代构造演化的一部分,东天山构造带从泥盆纪到二叠纪经历了一个完整的拉张、俯冲、碰撞造山及后碰撞演化阶段,是全球显生宙构造-岩浆事件以及陆壳增生最显著的地区(Chen *et al.*, 2007, 2012; Pirajno, 2009, 2013; 翟裕生等, 2011)。东天山陆壳增生和改造过程中,伴随着多期次、多类型的壳幔相互作用和多样性的成矿过程,沿康古尔韧性剪切带发育了大规模的石炭-二叠纪花岗岩类(李华芹等, 1998; 秦克章, 2000; 刘德权等, 2003; 陈富文等, 2005; 王龙生等, 2005; 吴昌志等, 2006; 陈文等, 2005; 郭谦谦等, 2010)和少量的泥盆纪(李亚萍等, 2006; 唐俊华等, 2007; 周涛发等, 2010)与三叠纪(李文明等, 2002; Zhang *et al.*, 2005; 周涛发等, 2010)花岗岩类,形成了铜、钼、金等金属元素超常富集的多类型成矿系统(Chen *et al.*, 2007, 2012; 翟裕生等, 2009, 2011; Deng *et al.*, 2011, 2013, 2014)。造就了土屋-延东铜矿、白山钼矿和康古尔金矿等一系列大型、超大型矿床。在东天山地壳增生和改造过程中,如何形成铜、钼、金等成矿金属元素的超常预富集,目前备受关注。

Hildreth and Moorbath(1988)、Hildreth(2007)和Richards(2003)提出了熔融-同化-贮存-均一化(MASH)模型,具体可以表述为幔源岩浆导致地壳部分熔融(melting),两种熔浆的相互混染(assimilation),然后其混合物被装载(storage)到某一空间因混合作用和化学扩散而均一化(homogenisation)。在部分熔融平衡体系中,含流体越多的熔浆表明其部分熔融程度越低,在熔融相图中位于固相线附近,是一种低温岩浆,低温饱和水熔浆是没有上侵能力的(Deng *et al.*, 2001, 2004, 2007; 罗照华等, 2007, 2008, 2010)。自然界最常见的含矿岩浆却是高温岩浆。例如,大部分含矿花岗岩斑岩仍保留有高温石英斑晶。这种特点一方面说明花岗岩斑岩岩浆是高温岩浆,另一方面说明花岗岩斑岩是岩浆快速上升、侵位、冷却、固结的结果(罗照华等, 2010; 罗照华, 2012)。这些研究成果可能对认识东天山地壳增生和改造过程中形成铜、钼、金等成矿金属元素的超常预富集具有重要启示。新疆东天山土屋-延东斑岩型铜矿床是东天山铜、钼、金等多金属成矿带的重要组成部分,对其开展研究,可为东天山造山带增生-改造过程与成矿作用研究提供宝贵的资料。

土屋和延东斑岩型铜矿床位于新疆东天山康古尔断裂以北,哈密市西南180km处(图1a)。土屋斑岩铜矿床是新疆地质勘查局第一地质大队1994年进行1:5万区调时发现的,1997年开展铜矿普查时取得了重大进展,随后又发现了延东、土屋东和延西等铜矿,构成了土屋-延东矿田(申萍等2012; 潘鸿迪等2013)。该矿田是新疆第一个大型斑岩型铜矿田,一经发现便引起了国内外地质学家的广泛关注,并开展了多方面的研究,取得了重要进展,包括成矿地质背

景(芮宗瑶等, 2002; 李锦轶, 2004; 王京彬和徐新, 2006; 申萍等, 2012)、矿床地质特征(王福同等, 2001; 芮宗瑶等, 2002; 刘德权等, 2003; 张连昌等, 2004; 李智明等, 2006; 张达玉等, 2010)、容矿岩石(任秉琛等, 2002; Han *et al.*, 2006; 侯广顺和杨贺杰, 2009; 申萍等, 2012; 潘鸿迪等, 2013)及成矿机制等方面(芮宗瑶等, 2002; 张连昌等, 2004; Han *et al.*, 2006; 郭谦谦等, 2010; 申萍等, 2012; Wang *et al.*, 2014a)。然而,这些研究对矿床若干重大地质问题,如成岩成矿时代和构造动力学背景的认识仍存在较大分歧(芮宗瑶等2002; 秦克章等2002; 刘德权等2003; 张连昌等2004; 陈富文等2005)。对岩石成因等研究较少。对这些问题的认识直接影响到对矿床的基本认识和今后的找矿普查方向(刘德权等2003)。造成这些分歧的原因,在很大程度上与缺乏系统的、高质量的年代学和地球化学数据有关。作为东天山造山带增生-改造过程与成矿作用研究的一部分,本文以土屋斑岩铜矿床为例,主要报道了该矿床含矿岩体的锆石 U-Pb 年代学、全岩元素地球化学和 Lu-Hf 同位素数据,并结合详细的野外地质调查和室内岩相学研究,对土屋斑岩铜矿床含矿岩体的成岩成矿时代、岩石成因和地球动力学背景进行了探讨,期望能有助于对土屋-延东矿田斑岩铜矿的深入研究。

1 地质背景及样品

1.1 区域地质概况

东天山多金属成矿带是我国最重要的 Au、Cu(Ni)、Fe 等矿产富集区之一(Han *et al.*, 2006),位于乌鲁木齐-库尔勒公路以东,吐哈盆地以南的天山地区。东天山主要包括三个构造单元,从北向南依次为:博格达-哈尔里克构造带、觉罗塔格构造带和中天山地块(Qin *et al.*, 2011)。觉罗塔格构造带又分为梧桐窝子-小热泉子岛弧带、大南湖-头苏泉岛弧带、康古尔-黄山韧性剪切带和阿奇山-雅满苏岛弧带(图1a)。区域断裂构造发育,自北向南依次有大草滩断裂、康古尔断裂、雅满苏断裂和阿奇克库都克断裂。大草滩断裂以北为下泥盆统大南湖组火山岩和中泥盆统头苏泉组沉积岩;康古尔断裂以南则出露石炭系干墩组 and 梧桐窝子组,为一套复理石建造,后期叠加强烈的韧性剪切变形;两条大断裂之间主要为石炭系企鵝山群,以中基性火山熔岩为主并夹少量碎屑岩(Yuan *et al.*, 2007)。区域发育了大规模的晚古生代花岗岩类,多呈岩株、岩枝或岩脉状产出,主要为华力西期的斜长花岗岩-花岗闪长岩-二长花岗岩系列和英云闪长岩、闪长玢岩。

1.2 矿床地质特征

土屋铜矿床位于东天山晚古生代大南湖-头苏泉岛弧带

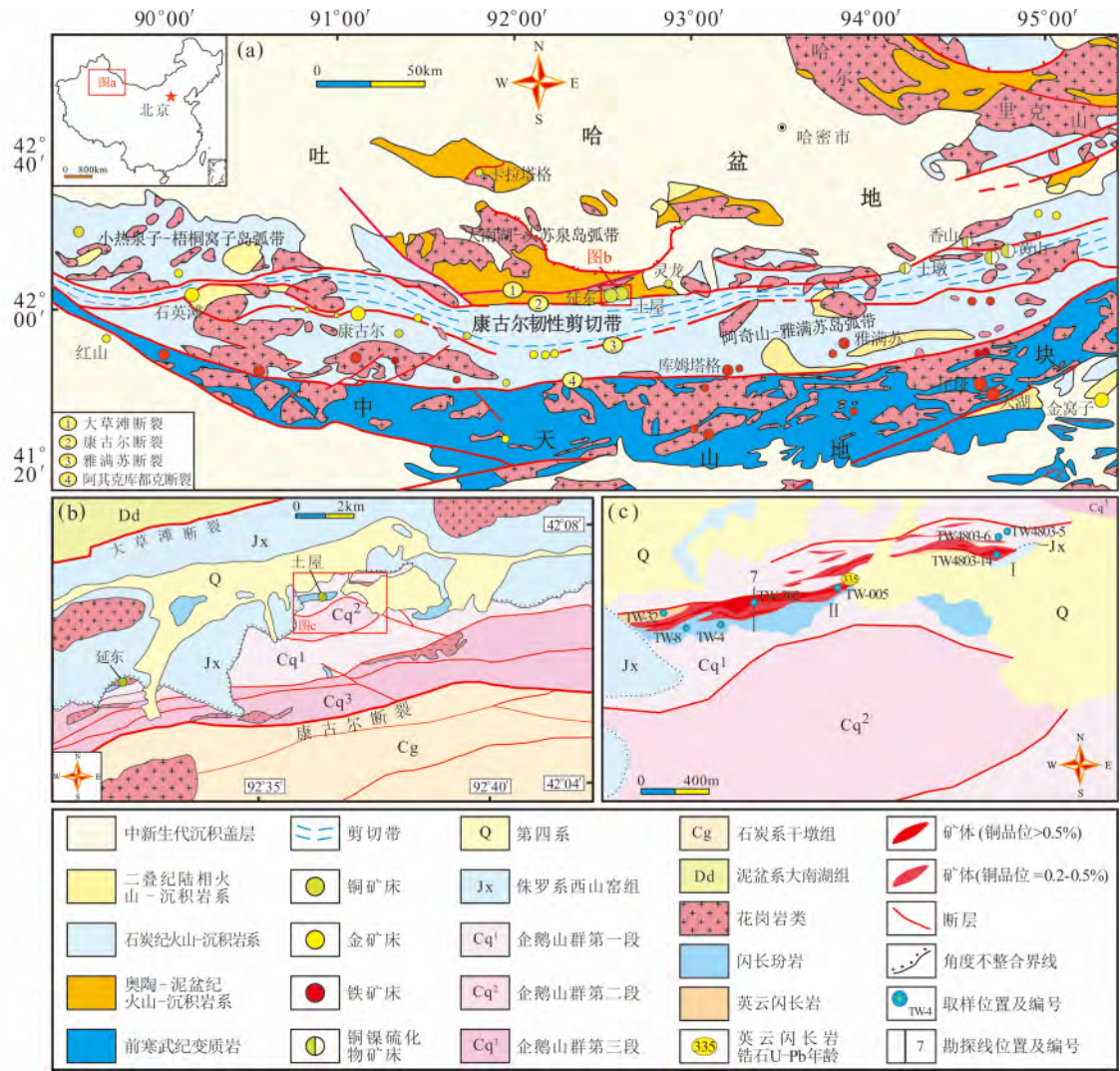


图1 新疆东天山大地构造图和研究区地质简图
(a) -新疆东天山大地构造图(据王京彬等 2006 修改); (b) -土屋-延东矿田地质简图(据申萍等 2012 修改); (c) -土屋斑岩铜矿区地质简图(据潘鸿迪等 2013 修改)

Fig.1 Tectonic map of the eastern Tianshan and geological sketch map
(a) -tectonic map of the eastern Tianshan (modified after Wang *et al.*, 2006); (b) -geological map of the Tuwu-Yandong ore field (modified after Shen *et al.*, 2012); (c) -geological sketch map of the Tuwu porphyry copper deposit (modified after Pan *et al.*, 2013)

中,分布于大草滩断裂与康古尔深大断裂之间,北距大草滩断裂约4.6km(图1b)。土屋铜矿床包括土屋和土屋东矿区,赋矿地层为下石炭统企鹅山群(Cq),主要划分为三个岩性组:第一岩性组(紧邻康古尔断裂分布)由陆内碎屑岩、沉凝灰岩组成;第二岩性组为玄武岩、安山岩等,夹英安岩和玄武安山岩;第三岩性组为砂岩、复成分砾岩及少量凝灰岩、安山岩等(王福同等 2001;李智明等 2006;吴兆宁等 2007)。地层总体走向为北东东向,倾向南,倾角43°~63°。侏罗系西山窑组(Jx)出露于矿区北部,岩性主要为砂岩、粉砂岩、泥岩及砾岩等。

矿区内岩浆侵入作用强烈,发育浅成、超浅成酸性岩体,多呈岩株、岩脉状侵入于石炭系企鹅山群玄武岩和安山

岩中,岩性主要为闪长玢岩及英云闪长岩(图1c)。闪长玢岩体呈不规则状NEE向展布,出露面积大于4km²,大部分被新生代沉积物覆盖,岩体特征与中基性火山岩相似,应属火山喷发末期浅火山(或浅成)岩浆上侵产物(王福同等, 2001),为主要赋矿围岩。英云闪长岩体呈不规则透镜状产出,走向近东西,剖面上为多个岩脉,出露面积小于0.03km²(王福同等 2001),为主要含矿岩石。矿区内东西向断裂发育,还有部分南北向、北西向断裂。

土屋铜矿床由两个矿体组成。I号矿体(即土屋东矿床)基本产于英云闪长岩中,以0.2×10⁻²为边界品位圈定矿体长1300m,宽约8.0~87.1m,地表平均铜品位为0.3%;II号矿体(即土屋矿床)位于I号矿体西段南侧,赋存于围岩

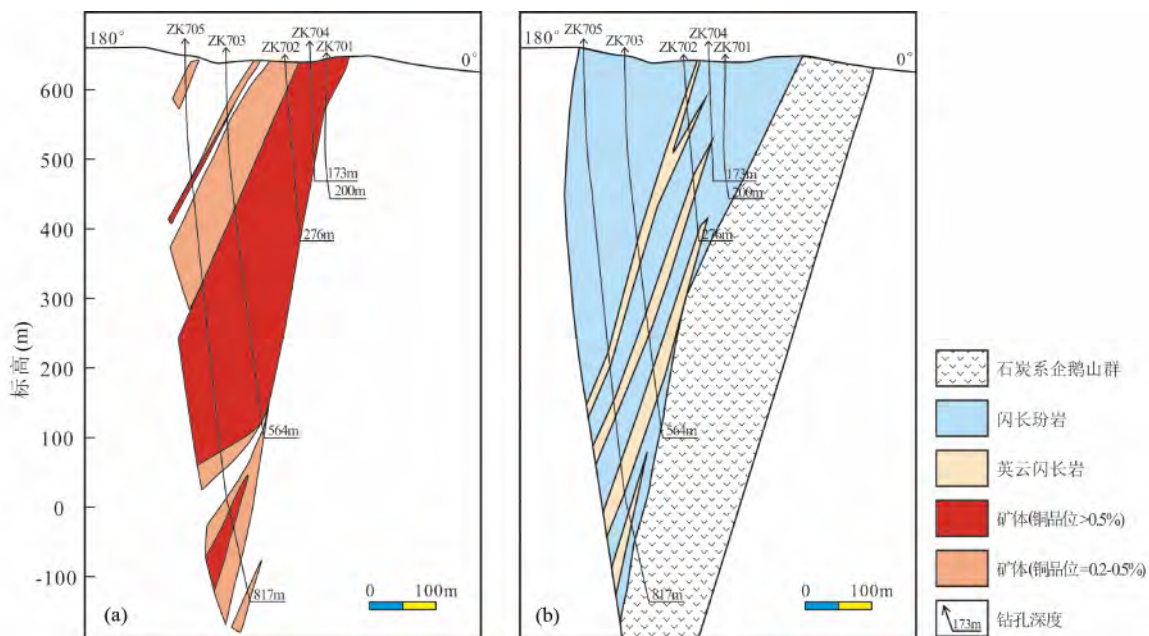


图2 土屋斑岩铜矿床7号勘探线矿体(a)和岩性(b)剖面图(据潘鸿迪等 2013 修改)

Fig.2 Cross section along No.7 exploration line with ore body (a) and lithologies (b) in the Tuwu porphyry copper deposit (modified after Pan *et al.*, 2013)

及英云闪长岩中,以 0.2×10^{-2} 为边界品位圈定矿化体长 1400m,宽约 7.6 ~ 125.0m,平均铜品位 0.44% (刘敏等, 2009)。土屋铜矿床 I、II 号矿体在平面上呈脉状,局部呈透镜状产出,走向近 EW,倾向南,倾角 $61^{\circ} \sim 67^{\circ}$ (图 2),铜品位一般为 $0.2 \times 10^{-2} \sim 0.7 \times 10^{-2}$,矿化与英云闪长岩有关(刘德权等, 2003; 张连昌等, 2004; Han *et al.*, 2006)。

矿石矿物成分简单,主要为黄铜矿,次为斑铜矿、黄铁矿、辉钼矿、铜蓝等;脉石矿物主要有石英、绢云母、绿泥石及黑云母等。矿石结构主要为中-细粒半自形-他形粒状结构,矿石构造为浸染状、肠状、细脉状、鳞片状及星点-稀疏浸染状。土屋铜矿床围岩蚀变发育,具“中心式”对称面型分带特征,以矿体为中心向两侧依次为石英带、黑云母化带、石英-绢云母带、泥化带及青盘岩化带(王福同等 2001)。

本文岩石样品均采自土屋铜矿区,所采岩石样品岩性分别为安山岩、闪长玢岩及英云闪长岩(图 3a, b)。安山岩为灰绿色和紫红色,斑状结构,主要矿物为斜长石以及少量的黑云母和角闪石,基质主要为石英、斜长石微晶以及少量隐晶质成分,岩石发生了硅化、绿帘石化、绢云母化和孔雀石化(图 3c)等蚀变。闪长玢岩呈灰绿色,具斑状结构,斑晶矿物主要为斜长石($An = 41 \sim 45$),斜长石呈自形-半自形柱状板状,粒径在 0.2 ~ 1.5mm 之间,有钠长石双晶现象,基质主要为斜长石的微晶和少量隐晶质成分;次生变化为绿泥石化、绢云母化及矿化作用叠加的硅化、碳酸盐化等。英云闪长岩具斑状结构,块状构造(图 3d),斑晶为斜长石($An = 30 \sim 40$)、石英及少量的黑云母;基质为花岗结构,由斜长石、石英及少量黑云母组成;次生变化为绢云母化和碳酸盐化(图

3e);矿石矿物主要含黄铜矿,呈浸染状分布(图 3f)。在土屋矿区,英云闪长岩为浅成侵入岩,切穿闪长玢岩岩株。

2 分析方法

锆石单矿物分选是在河北廊坊区域地质调查研究所通过浮选和电磁选的方法获得。在双目镜下观察分选好的锆石,将晶形好、无裂隙和包裹体的锆石挑出,用环氧树脂制靶。将锆石靶打磨抛光,然后进行反射光、透射光显微照相和阴极发光(CL)分析。锆石阴极发光(CL)显微照相是在中国地质科学院地质研究所电子探针室完成。锆石 U-Pb 同位素定年在中国科学院地质与地球物理研究所离子探针实验室完成,所用仪器为 Cameca IMS-4280 型双离子源多接收器二次离子质谱仪(SIMS)。SIMS 锆石 U-Pb 定年的详细分析流程见 Li *et al.* (2009),用强度为 10nA 一次 O_2^+ 离子束通过 -13kV 加速电压轰击样品表面,斑束约为 $20\mu m \times 30\mu m$ 。用非放射性 ^{204}Pb 校正普通铅,由于测得的普通 Pb 含量非常低,假定普通 Pb 主要来源于制样过程中带入的表面 Pb 污染,以现代地壳的平均 Pb 同位素组成(Stacey and Kramers, 1975)作为普通 Pb 组成进行校正。单一分析数据的误差为 1σ ,加权平均年龄计算采用 $^{206}Pb/^{238}U$ 表面年龄数据,其置信水平 95%。数据结果处理采用 ISOPLLOT 软件(Ludwig, 2001)。

主量元素和微量元素分析测试工作在中国核工业北京地质研究院分析测试研究中心完成。其中主量元素分析使用 Philips PW2404 型 X 荧光光谱仪(XRF)完成,分析精度优

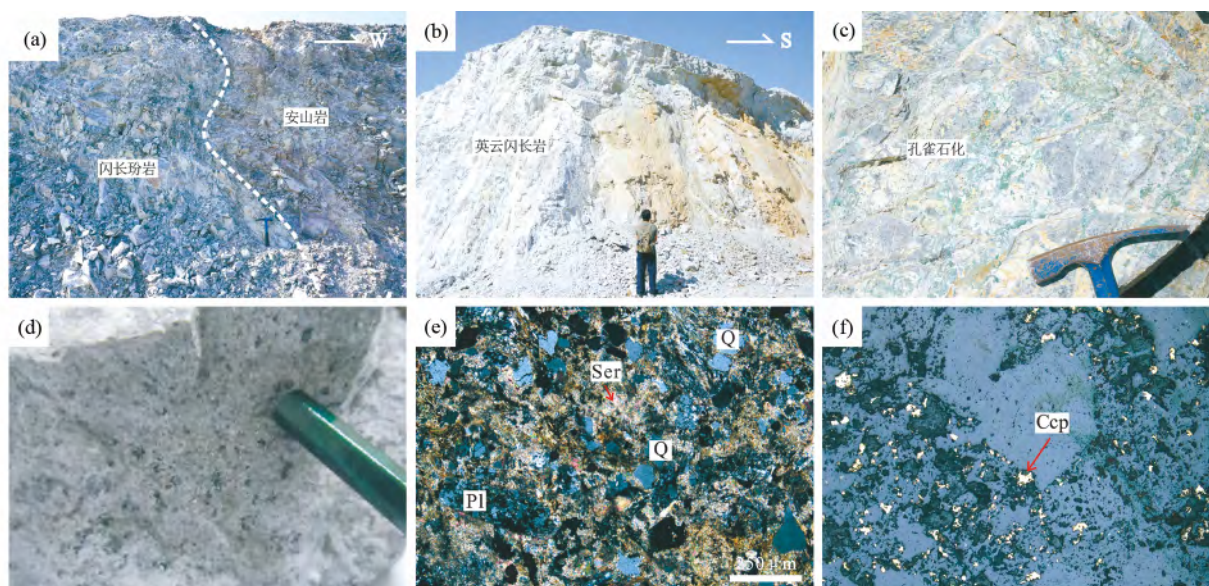


图3 土屋斑岩铜矿区、手标本及显微镜下照片

(a) -地表闪长玢岩、安山岩; (b) -地表英云闪长岩; (c) -孔雀石化; (d) -英云闪长岩; (e) -英云闪长岩, 具斑状结构, 斑晶主要为石英、斜长石, 可见绢云母化、碳酸盐化, 正交偏光; (f) -浸染状黄铜矿。矿物缩写: Pl-斜长石; Ser-绢云母; Q-石英; Ccp-黄铜矿

Fig. 3 Representative field photos, hand specimen photo and microphotographs from the Tuwu porphyry copper deposit

(a) -diorite porphyrite and andesite in Tuwu area; (b) -tonalitic rocks in Tuwu area; (c) -malachitization; (d) -the hand specimen of tonalitic rock; (e) -microphotograph of tonalitic rock, the phenocrysts are quartz and plagioclase, showing sericitization and carbonatation, CPL; (f) -disseminated chalcopyrite with xenomorphic granular, CPL. Abbreviations: Pl-plagioclase; Ser-sericite; Q-quartz; Ccp-chalcopyrite

于1%; 微量元素分析使用德国 Finnigan MAT 公司生产的 Element I 型电感耦合等离子体质谱仪 (ICP-MS) 完成, 分析精度多小于3%。

锆石 Lu-Hf 同位素测试是在中国地质科学院矿产资源研究所国土资源部成矿作用与资源评价重点实验室 Neptune 多接收电感耦合等离子质谱仪 (MC-ICPMS) 和 Newwave UP213 紫外激光剥蚀系统 (LA-MC-ICP-MS) 上进行的, 实验过程中采用 He 作为剥蚀物质载气, 剥蚀直径 55 μ m 或 40 μ m, 测定时使用锆石国际标样 GJ-1 作为参考物质, 分析点与锆石 U-Pb 定年点位置相同。相关仪器运行条件及详细分析流程见侯可军等 (2007)。分析过程中, 锆石标准 GJ-1 的 $^{176}\text{Hf}/^{177}\text{Hf}$ 加权平均值为 0.282007 ± 0.000007 ($2\sigma, n=36$), 与文献报道值 (侯可军等, 2007; Morel *et al.*, 2008) 在误差范围内一致。 $\varepsilon_{\text{Hf}}(t)$ 根据每个测点的锆石 U-Pb 年龄计算, 采用的 ^{176}Lu 衰变常数为 $1.867 \times 10^{-11} \text{a}$ (Soderlund *et al.*, 2004), 利用平均大陆壳的 $^{176}\text{Lu}/^{177}\text{Hf}$ 值 ($=0.015$) 计算锆石 Hf 同位素地壳模式年龄 (t_{DM}^{C})。

3 分析结果

3.1 锆石 U-Pb 年龄

锆石样品分选自英云闪长岩代表性样品 TW-005, 采自土屋矿区 II 号矿体。本文对样品 TW-005 进行了 SIMS 锆石

U-Pb 定年, 分析结果见表 1。锆石多为无色长柱状晶形, 长宽比约为 2:1~4:1, 发育清晰的振荡环带 (图 4a)。锆石的 Th 含量为 $21 \times 10^{-6} \sim 134 \times 10^{-6}$, U 含量 $54 \times 10^{-6} \sim 208 \times 10^{-6}$, Th/U 比值为 0.36~0.70, 与变质成因锆石 Th/U 值 (通常小于 0.1) 明显不同, 属于典型的岩浆锆石特征 (Hoskin and Schaltegger, 2003)。在 $^{206}\text{Pb}/^{238}\text{U}$ 和 $^{207}\text{Pb}/^{235}\text{U}$ 谐和图上 (图 4b), 除第 3、4、6、9 等 4 个测点外, 其余 11 个测点均靠近 U-Pb 谐和线, $^{206}\text{Pb}/^{238}\text{U}$ 年龄范围为 331.6~339.9Ma, 加权平均年龄为 $334.7 \pm 3.0 \text{Ma}$ (MSWD=0.18), 代表了英云闪长岩的结晶年龄。

3.2 全岩地球化学

土屋斑岩铜矿的安山岩、闪长玢岩和英云闪长岩的主量、微量和稀土元素分析数据见表 2。安山岩 SiO_2 含量为 53.90%~54.04%, Al_2O_3 含量为 17.42%~17.72%, K_2O 与 Na_2O 含量分别为 0.71%~1.14% 和 2.92%~3.90%。闪长玢岩 SiO_2 含量为 56.28%~56.98%, Al_2O_3 含量为 16.41%~16.70%, K_2O 与 Na_2O 含量分别为 0.58%~0.83% 和 2.60%~4.15%。英云闪长岩 SiO_2 含量为 64.58%~67.35%, Al_2O_3 含量 14.42%~19.03%, K_2O 与 Na_2O 含量分别为 0.87%~3.09% 和 1.67%~4.33%。土屋斑岩铜矿床岩石样品全碱 ($\text{Na}_2\text{O} + \text{K}_2\text{O}$) 含量为 3.18%~6.22%, 在 TAS 图解中, 安山岩和闪长玢岩样品落入玄武安山岩-安山岩区域内, 英云闪长岩样品全部落入英安岩区域内 (图 5a); 在

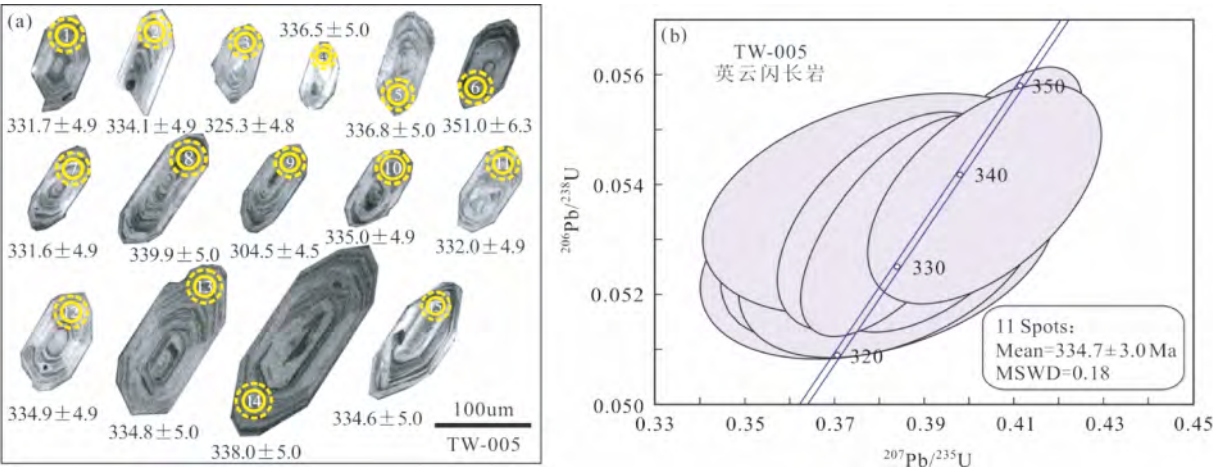


图4 土屋英云闪长岩锆石阴极发光(CL) 图像(a) 和 U-Pb 年龄谐和图(b)

Fig. 4 Cathodoluminescence (CL) image of representative zircons (a) and concordia diagram (b) for zircons from Tuwu tonalitic rocks

表1 东天山土屋地区岩浆岩 SIMS 锆石 U-Pb 定年数据

Table 1 SIMS zircon U-Pb analysis data of magmatic rocks in the Tuwug area of eastern Tianshan

测点号	²⁰⁶ Pb _c (%)	U (× 10 ⁻⁶)	Th (× 10 ⁻⁶)	Th/U	²⁰⁶ Pb [*] (× 10 ⁻⁶)	同位素比值								²⁰⁶ Pb _{238U}	± 1σ
						²³⁸ U ²⁰⁶ Pb [*]	± 1σ	²⁰⁷ Pb [*] ²⁰⁶ Pb [*]	± 1σ	²⁰⁷ Pb [*] ²³⁵ U	± 1σ	²⁰⁶ Pb [*] ²³⁸ U	± 1σ	(Ma)	
						TW-005: 英云闪长岩, 11 个测点(不包括第 3、4、6、9 测点) 加权平均年龄: 334. 7 ± 3. 0Ma(MSWD = 0. 18)									
TW-005@01	0. 91	74	38	0. 51	4. 69	18. 9374	1. 5283	0. 0522	4. 0276	0. 3799	4. 3078	0. 0528	1. 5283	331. 7	4. 9
TW-005@02	0. 58	125	58	0. 46	7. 82	18. 8015	1. 5070	0. 0509	2. 6977	0. 3730	3. 0901	0. 0532	1. 5070	334. 1	4. 9
TW-005@03	1. 43	143	86	0. 60	9. 03	19. 3224	1. 5008	0. 0525	3. 2602	0. 3749	3. 5890	0. 0518	1. 5008	325. 3	4. 8
TW-005@04	3. 81	54	21	0. 40	3. 24	18. 6594	1. 5312	0. 0396	12. 0447	0. 2924	12. 1416	0. 0536	1. 5312	336. 5	5. 0
TW-005@05	1. 04	71	35	0. 50	4. 57	18. 6471	1. 5276	0. 0516	4. 1034	0. 3812	4. 3785	0. 0536	1. 5276	336. 8	5. 0
TW-005@06	1. 09	65	29	0. 44	4. 36	17. 8705	1. 8491	0. 0509	3. 6180	0. 3929	4. 0631	0. 0560	1. 8491	351. 0	6. 3
TW-005@07	0. 59	113	80	0. 70	7. 55	18. 9456	1. 5038	0. 0526	3. 2636	0. 3826	3. 5934	0. 0528	1. 5038	331. 6	4. 9
TW-005@08	0. 13	208	134	0. 65	14. 14	18. 4694	1. 5001	0. 0541	1. 5891	0. 4037	2. 1853	0. 0541	1. 5001	339. 9	5. 0
TW-005@09	0. 14	75	30	0. 39	4. 24	20. 6769	1. 5074	0. 0533	1. 6189	0. 3555	2. 2121	0. 0484	1. 5074	304. 5	4. 5
TW-005@10	0. 38	102	55	0. 54	6. 62	18. 7474	1. 5074	0. 0519	2. 1821	0. 3820	2. 6522	0. 0533	1. 5074	335. 0	4. 9
TW-005@11	0. 28	91	33	0. 36	5. 64	18. 9238	1. 5083	0. 0529	3. 0403	0. 3854	3. 3939	0. 0528	1. 5083	332. 0	4. 9
TW-005@12	0. 20	116	75	0. 65	7. 79	18. 7514	1. 5094	0. 0535	1. 6873	0. 3932	2. 2639	0. 0533	1. 5094	334. 9	4. 9
TW-005@13	0. 23	76	40	0. 53	4. 93	18. 7592	1. 5167	0. 0535	2. 2037	0. 3935	2. 6752	0. 0533	1. 5167	334. 8	5. 0
TW-005@14	0. 28	71	46	0. 64	4. 79	18. 5787	1. 5053	0. 0544	2. 2168	0. 4036	2. 6796	0. 0538	1. 5053	338. 0	5. 0
TW-005@15	0. 21	103	57	0. 55	6. 71	18. 7718	1. 5392	0. 0523	1. 7823	0. 3843	2. 3550	0. 0533	1. 5392	334. 6	5. 0

注: ²⁰⁶Pb_c(%) 指普通²⁰⁶Pb 在全部²⁰⁶Pb 中的百分数; ²⁰⁶Pb* 指放射性成因铅; 普通铅用²⁰⁴Pb 校正

K₂O-SiO₂ 图解中,显示样品均属于钙碱性到高钾钙碱性系列岩石(图 5b)。土屋斑岩铜矿床岩石样品的铝饱和指数(A/ CNK) 为 0.90 ~ 2.84,指示为偏铝质到过铝质岩石(图 5c)。样品的 SiO₂ 与 P₂O₅、MnO、Fe₂O₃^T、MgO、CaO、Al₂O₃ 等都呈良好的线性关系(图 6)。

安山岩的稀土总量均值为 88.97 × 10⁻⁶,闪长玢岩的稀土总量均值为 58.43 × 10⁻⁶,英云闪长岩的稀土总量均值为 51.87 × 10⁻⁶。在稀土元素球粒陨石标准化配分图中,所有样品均表现轻稀土富集,重稀土亏损(Yb = 0.75 × 10⁻⁶ ~ 2.49 × 10⁻⁶)。轻重稀土分异明显(图 7a),其中英云闪长岩较安山岩及闪长玢岩分异更明显。所有岩石样品轻重稀土比值(LREE/HREE) 为 6.15 ~ 12.48,均值为 8.26; (La/Yb)_N

变化范围在 3.37 ~ 9.34 之间,均值为 5.40。除安山岩样品 TW4803-6 及英云闪长岩样品 TW32 外,其余样品均显示弱的正 Eu 异常(δEu = 1.00 ~ 1.14)。在微量元素原始地幔标准化蜘蛛图解中,安山岩、闪长玢岩及英云闪长岩样品均显示相似的特征,均富集 K、Rb、Sr、Ba 等大离子亲石元素(LILE) 相对亏损 Nb、Ta、Ti、Th 等高场强元素(HFSE),明显富集 U 和 Pb(图 7b)。

3.3 锆石 Hf 同位素数据

土屋英云闪长岩锆石 Hf 同位素测试是在 U-Pb 定年的基础上进行的。样品 TW-005 的 15 个锆石测点的数据结果列于表 3。不考虑测点 3、4、6 和 9,剩余 11 个锆石测点的¹⁷⁶Hf/

表2 东天山土屋地区岩浆岩全岩地球化学数据(主量元素 wt%; 微量元素 $\times 10^{-6}$)Table 2 Major (wt%) and trace ($\times 10^{-6}$) element chemistry of magmatic rocks in the Tuwu area of eastern Tianshan

样品号	TW4803-5	TW4803-6	TW-8	TW-4	TW-702	TW4803-14	TW32	Btw38 ^{a)}	TW33 ^{b)}	TW208 ^{b)}	TW-28 ^{c)}
岩石类型	安山岩	安山岩	闪长玢岩	闪长玢岩	英云闪长岩	英云闪长岩	英云闪长岩	英云闪长岩	英云闪长岩	英云闪长岩	安山岩
SiO ₂	53.90	54.04	56.28	56.98	67.35	65.71	64.58	64.34	69.76	68.21	53.21
TiO ₂	0.89	0.95	0.92	0.94	0.44	0.30	1.02	0.47	0.40	0.37	1.05
Al ₂ O ₃	17.42	17.72	16.70	16.41	14.42	15.24	19.03	17.71	15.89	17.08	17.46
Fe ₂ O ₃ ^T	7.70	7.80	9.07	7.18	2.50	5.99	2.43	4.397	2.27	1.84	8.57
MnO	0.09	0.09	0.03	0.07	0.03	0.04	0.03	0.04	0.03	0.03	0.10
MgO	5.57	4.52	5.18	4.53	1.50	1.33	3.90	2.20	1.28	1.35	5.10
CaO	5.32	7.53	3.58	5.79	3.14	1.80	0.69	2.30	1.22	1.56	5.37
Na ₂ O	3.90	2.92	2.60	4.15	4.33	1.67	2.75	4.60	4.93	4.89	3.90
K ₂ O	0.71	1.14	0.58	0.83	1.89	3.09	0.87	1.93	1.56	2.00	1.31
P ₂ O ₅	0.24	0.30	0.23	0.30	0.15	0.15	0.29	0.2	0.30	0.12	0.39
LOI	3.92	2.74	4.64	2.77	4.05	4.33	4.25	1.56	2.30	2.52	3.43
Total	99.65	99.74	99.81	99.95	99.80	99.65	99.84	99.75	99.94	99.97	99.90
A/CNK	1.03	0.90	1.46	0.90	0.97	1.62	2.83	1.28	1.32	1.31	0.99
A/NK	2.43	2.93	3.40	2.12	1.57	2.50	3.48	1.83	1.62	1.67	2.23
Mg [#]	59	54	53	56	55	31	76	50	53	59	54
FeO ^T	4.79	4.52	6.71	3.65	1.00	0.98	1.88	1.97	1.05	1.31	5.19
Li	13.50	11.10	9.66	7.41	4.39	7.49	16.30				17.20
Be	0.89	1.17	0.75	0.84	0.53	1.35	0.99				1.19
Sc	19.90	24.60	19.50	24.30	7.18	5.19	19.30				21.30
V	183	200	194	186	60.3	31.8	165				199
Cr	114	80.6	115	64.6	4.59	6.60	132		17.9	15.7	79.5
Co	32.70	25.80	28.30	18.60	5.92	23.00	5.33		12.80	6.06	26.20
Ni	1220	80.1	98.6	52.8	17.1	6.97	64.7			2.70	64.3
Cu	1240	540	384	13.6	7437	116	659				16.8
Zn	61.5	41.1	42.4	55.2	35.2	35.7	37.3				64.0
Ga	16.30	18.90	18.90	16.20	11.70	14.40	14.40				15.10
Rb	17.6	33.0	13.3	21.4	33.2	69.8	19.4	28.1	11.5	46.6	24.7
Sr	562	898	339	965	290	416	381	405	421	619	691
Y	15.90	24.40	12.70	18.40	7.73	8.70	13.40	7.90	6.30	6.17	20.10
Zr	81.7	156	102	157	33.4	44.9	88.7	100	86.7	41.9	200
Nb	2.91	4.67	2.60	3.70	1.98	2.30	3.27	2.70	2.18	3.15	4.34
Cs	2.84	3.88	1.72	3.32	2.03	4.25	1.31		0.46	3.57	4.26
Ba	108	180	74.0	96.0	82.8	553	55.1	394	458	1483	250
La	8.66	19.40	7.58	8.74	7.83	11.80	7.19	10.30	7.33	11.40	18.70
Ce	19.60	44.00	16.50	21.60	16.90	23.30	17.20	18.60	15.20	23.50	40.30
Pr	2.75	5.97	2.39	3.24	2.26	2.86	2.59		1.77	2.78	5.74
Nd	12.50	26.10	11.80	15.30	9.66	11.80	11.70	10.10	6.86	11.00	25.90
Sm	2.97	5.27	2.76	3.63	2.02	2.15	2.68	2.30	1.39	1.93	5.14
Eu	0.95	1.55	0.85	1.32	0.70	0.71	0.74	0.75	0.54	0.81	1.61
Gd	2.86	4.91	2.34	3.60	1.77	1.85	2.60	1.96	1.25	1.60	4.26
Tb	0.51	0.82	0.43	0.65	0.30	0.30	0.46	0.28	0.19	0.20	0.75
Dy	3.11	4.74	2.25	3.85	1.61	1.66	2.57		1.06	1.11	3.76
Ho	0.60	0.91	0.46	0.70	0.29	0.29	0.51		0.22	0.21	0.72
Er	1.75	2.66	1.18	1.90	0.79	0.93	1.41		0.65	0.59	2.00
Tm	0.26	0.38	0.20	0.29	0.12	0.13	0.23		0.11	0.08	0.32
Yb	1.63	2.49	1.18	1.72	0.75	0.91	1.53	0.84	0.70	0.59	2.03
Lu	0.24	0.36	0.17	0.24	0.12	0.14	0.23	0.14	0.12	0.08	0.28
Hf	2.23	4.01	2.48	4.21	0.94	1.59	2.48	1.75	2.29	1.23	5.11
Ta	0.20	0.32	0.19	0.51	0.23	0.21	0.24	0.19	0.21	0.32	0.27
Pb	8.95	1.88	5.77	3.74	4.59	14.20	3.87				6.29
Th	0.87	2.00	0.56	1.50	0.68	1.28	0.99	0.75		1.60	1.24
U	1.29	1.75	0.77	0.81	0.21	0.75	11.50			0.41	0.49

注: LOI 为烧失量; Fe₂O₃^T 为全铁, FeO^T = 0.9 × Fe₂O₃^T; Mg[#] = 100 × Mg²⁺ / (Mg²⁺ + Fe²⁺); A/CNK = 摩尔数 Al₂O₃ / (CaO + Na₂O + K₂O), A/NK = 摩尔数 Al₂O₃ / (Na₂O + K₂O); 数据来源: a) 李文明等 2002 b) 张连昌等 2004 c) 赵泽南 2014 其它为本文资料

表3 东天山土屋地区岩浆岩锆石 Hf 同位素数据

Table 3 Hf isotopic data for zircons from magmatic rocks in the Tuwu area of eastern Tianshan

测点号	年龄 (Ma)	$\frac{^{176}\text{Yb}}{^{177}\text{Hf}}$	$\frac{^{176}\text{Hf}}{^{177}\text{Hf}}$	$\pm 2\sigma$	$\frac{^{176}\text{Lu}}{^{177}\text{Hf}}$	$\frac{^{176}\text{Hf}}{^{177}\text{Hf}}$ (t)	$\frac{^{176}\text{Hf}}{^{177}\text{Hf}}$ CHUR(T)	$\varepsilon_{\text{Hf}}(0)$	$\varepsilon_{\text{Hf}}(t)$	t_{DM} (Ma)	t_{DM}^{C} (Ma)	$f_{\text{Lu/Hf}}$
TW-005: 英云闪长岩 $334.7 \pm 3.0\text{Ma}$ (MSWD = 0.18) (11 个测点, 不包括第3、4、6、9 测点) $\varepsilon_{\text{Hf}}(t) = 6.3 \sim 16.1$												
TW-005-01	331.7	0.083310	0.282792	0.000063	0.002515	0.282776	0.282566	0.7	7.4	680	865	-0.92
TW-005-02	334.1	0.081412	0.282981	0.000037	0.002188	0.282967	0.282564	7.4	14.3	396	431	-0.93
TW-005-03	325.3	0.107147	0.282902	0.000052	0.002411	0.282887	0.282570	4.6	11.2	516	619	-0.93
TW-005-04	336.5	0.090940	0.283222	0.000122	0.003311	0.283201	0.282563	15.9	22.6	42	104	-0.90
TW-005-05	336.8	0.066610	0.282853	0.000035	0.002157	0.282839	0.282563	2.9	9.8	584	719	-0.94
TW-005-06	351.0	0.130745	0.283020	0.000042	0.004249	0.282992	0.282554	8.8	15.5	360	364	-0.87
TW-005-07	331.6	0.073937	0.282922	0.000045	0.002257	0.282908	0.282566	5.3	12.1	484	566	-0.93
TW-005-08	339.9	0.072102	0.282865	0.000036	0.002110	0.282852	0.282561	3.3	10.3	565	689	-0.94
TW-005-09	304.5	0.073916	0.282815	0.000046	0.001963	0.282804	0.282583	1.5	7.8	636	820	-0.94
TW-005-10	335.0	0.062855	0.282822	0.000032	0.001921	0.282810	0.282564	1.8	8.7	624	786	-0.94
TW-005-11	332.0	0.077830	0.283035	0.000035	0.002167	0.283022	0.282566	9.3	16.1	317	308	-0.93
TW-005-12	334.9	0.062525	0.282757	0.000057	0.002177	0.282743	0.282564	-0.5	6.3	725	938	-0.93
TW-005-13	334.8	0.066622	0.283017	0.000040	0.002029	0.283004	0.282564	8.7	15.6	342	346	-0.94
TW-005-14	338.0	0.068293	0.283022	0.000038	0.002090	0.283009	0.282562	8.8	15.8	336	334	-0.94
TW-005-15	334.6	0.045253	0.282876	0.000037	0.001534	0.282866	0.282564	3.7	10.7	541	660	-0.95

注: $\varepsilon_{\text{Hf}}(t) = 10000 \times \left(\left\{ \left[\frac{^{176}\text{Hf}}{^{177}\text{Hf}} \right]_{\text{S}} - \left(\frac{^{176}\text{Lu}}{^{177}\text{Hf}} \right)_{\text{S}} \times (e^{\lambda t} - 1) \right\} / \left[\left(\frac{^{176}\text{Hf}}{^{177}\text{Hf}} \right)_{\text{CHUR}} - \left(\frac{^{176}\text{Lu}}{^{177}\text{Hf}} \right)_{\text{CHUR}} \times (e^{\lambda t} - 1) \right] - 1 \right)$. $t_{\text{DM}} = 1 / \lambda \times \ln \{ 1 + \left[\left(\frac{^{176}\text{Hf}}{^{177}\text{Hf}} \right)_{\text{S}} - \left(\frac{^{176}\text{Hf}}{^{177}\text{Hf}} \right)_{\text{DM}} \right] / \left[\left(\frac{^{176}\text{Hf}}{^{177}\text{Hf}} \right)_{\text{S}} - \left(\frac{^{176}\text{Hf}}{^{177}\text{Hf}} \right)_{\text{DM}} \right] \}$. $t_{\text{DM}}^{\text{C}} = t_{\text{DM}} - (t_{\text{DM}} - t) \times \left[(f_{\text{cc}} - f_{\text{s}}) / (f_{\text{cc}} - f_{\text{DM}}) \right]$. $f_{\text{Lu/Hf}} = \left(\frac{^{176}\text{Lu}}{^{177}\text{Hf}} \right)_{\text{S}} / \left(\frac{^{176}\text{Lu}}{^{177}\text{Hf}} \right)_{\text{CHUR}} - 1$. 其中: $\lambda = 1.867 \times 10^{-11} / \text{a}$ (Soderlund *et al.*, 2004); $\left(\frac{^{176}\text{Lu}}{^{177}\text{Hf}} \right)_{\text{S}}$ 和 $\left(\frac{^{176}\text{Hf}}{^{177}\text{Hf}} \right)_{\text{S}}$ 为样品测量值; $\left(\frac{^{176}\text{Lu}}{^{177}\text{Hf}} \right)_{\text{CHUR}} = 0.0332$, $\left(\frac{^{176}\text{Hf}}{^{177}\text{Hf}} \right)_{\text{CHUR},0} = 0.282772$ (Blichert-Toft and Albarède, 1997); $\left(\frac{^{176}\text{Lu}}{^{177}\text{Hf}} \right)_{\text{DM}} = 0.0384$, $\left(\frac{^{176}\text{Hf}}{^{177}\text{Hf}} \right)_{\text{DM}} = 0.28325$ (Griffin *et al.*, 2000); $\left(\frac{^{176}\text{Lu}}{^{177}\text{Hf}} \right)_{\text{平均地壳}} = 0.015$; $f_{\text{cc}} = \left[\left(\frac{^{176}\text{Lu}}{^{177}\text{Hf}} \right)_{\text{mean crust}} / \left(\frac{^{176}\text{Lu}}{^{177}\text{Hf}} \right)_{\text{CHUR}} \right] - 1$; $f_{\text{s}} = f_{\text{Lu/Hf}}$; $f_{\text{DM}} = \left[\left(\frac{^{176}\text{Lu}}{^{177}\text{Hf}} \right)_{\text{DM}} / \left(\frac{^{176}\text{Lu}}{^{177}\text{Hf}} \right)_{\text{CHUR}} \right] - 1$; t 为锆石结晶年龄

^{177}Hf 变化在 0.282757 ~ 0.283035 之间, 对应的 $\varepsilon_{\text{Hf}}(t)$ 值为 6.3 ~ 16.1, 位于亏损地幔演化线附近, 由此指示英云闪长岩的岩浆源区可能来自俯冲板片的部分熔融 (Chung *et al.*, 2003; 熊小林等, 2005; Wen *et al.*, 2008; 罗照华等, 2010; He *et al.*, 2011; Guan *et al.*, 2011; 朱志敏等, 2013)。样品的 Hf 同位素亏损地幔模式年龄平均为 498Ma, 这比锆石的平均 U-Pb 年龄 (335Ma) 略大, 进一步说明岩浆物质可能来源于俯冲板片的部分熔融。

4 讨论

4.1 成岩成矿时代

已有资料表明, 东天山地区花岗岩类主要产于 386 ~ 230Ma 之间, 岩浆活动可分为晚泥盆世 (386 ~ 369Ma) (Zhou *et al.*, 2008; Wang *et al.*, 2009)、早石炭世 (349 ~ 330Ma) (王京彬和徐新, 2006; 顾连兴等, 2006; Zhou *et al.*, 2008)、晚石炭世-晚二叠世 (320 ~ 252Ma) (王京彬和徐新, 2006; 韩宝福等, 2006; 姜峰和喻亨祥, 2007) 和早中三叠世 (246 ~ 230Ma) (Sylvester, 1998; 刘新秒, 2000; 顾连兴等, 2006; Zhou *et al.*, 2008) 等 4 个阶段。前 3 个阶段岩浆活动具有持续时间逐渐变长、岩浆活动逐渐加剧的特点, 并在第三阶段达到顶峰, 而第四阶段岩浆活动则明显变弱。花岗岩

类岩浆活动在时空分布上表现为: 自哈尔里克-大南湖岛弧带-阿奇山-雅满苏岛弧带-康古尔韧性剪切带, 岩体侵位由早到晚; 自东天山东部-中西部-沿康古尔韧性剪切带, 岩体侵位由老到新。与 4 个阶段花岗岩类岩浆活动有关的成矿作用由早到晚表现为无明显矿化-斑岩型铜矿-火山岩型铁矿-韧性剪切带型金矿、夕卡岩型银 (铜) 矿-斑岩-石英脉型钼矿的演化特点, 其中以斑岩型铜矿和韧性剪切带型金矿最为发育 (周涛发等, 2010; Wang *et al.*, 2014a)。

本文对土屋英云闪长岩的锆石矿物颗粒的标型内部结构研究表明, 锆石颗粒较大, 晶型完好, 成分单一, 具有典型的岩浆型锆石韵律环带结构 (图 4a), 说明锆石是在岩浆系统中结晶形成。本次获得土屋英云闪长岩的 SIMS 锆石 U-Pb 年龄值为 $334.7 \pm 3.0\text{Ma}$, 代表了土屋英云闪长岩岩浆结晶年代, 说明土屋地区英云闪长岩形成时限为早石炭世。该结论与刘德权等 (2003)、陈富文等 (2005)、郭谦谦等 (2010) 和 Wang *et al.* (2014b) 获得的土屋-延东铜矿床含矿英云闪长岩的成岩年代在 340 ~ 330Ma 一致。

对于成矿时代, 芮宗瑶等 (2002) 获得了土屋-延东铜矿床 323Ma 的辉钼矿 Re-Os 年龄; 秦克章等 (2002) 测得土屋-延东矿区内蚀变绢云母 K-Ar 年龄为 341Ma; 张连昌等 (2004) 测得延东矿区细脉浸染状的辉钼矿 Re-Os 年龄为 343Ma; 张达玉等 (2010) 测得延西铜矿床辉钼矿 Re-Os 年龄

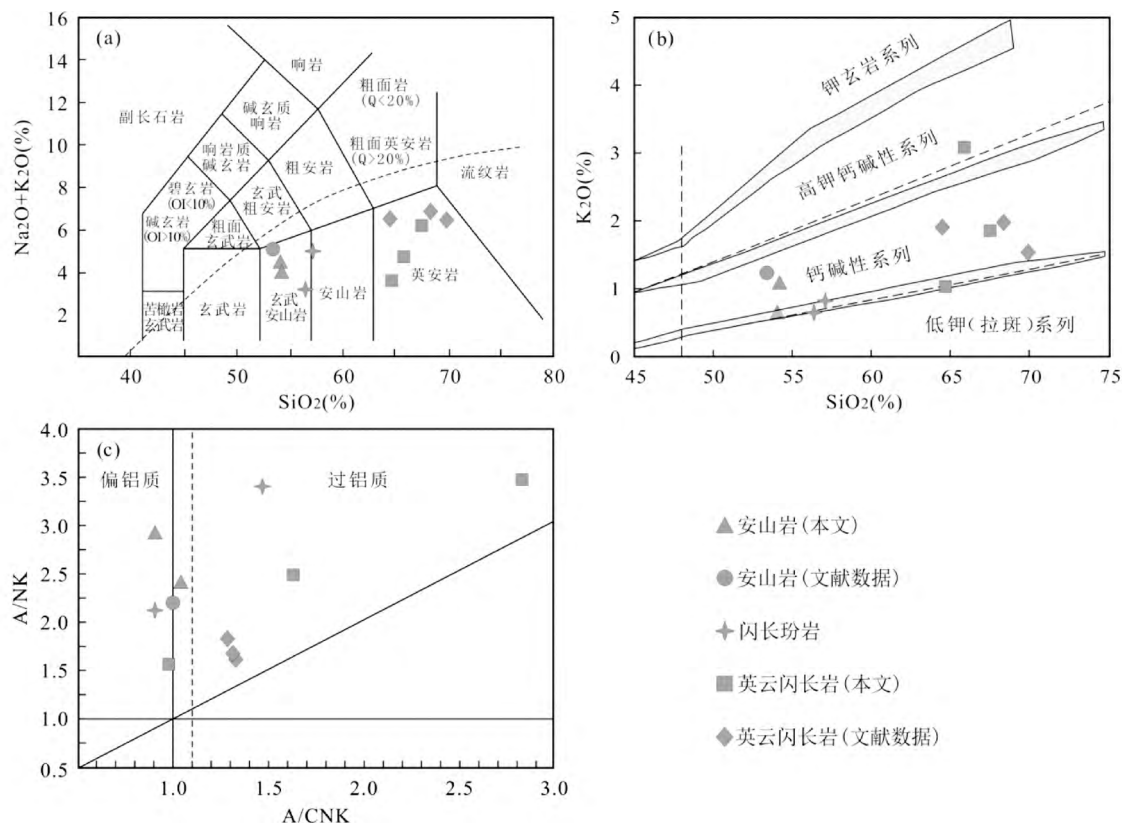


图5 土屋主要岩石类型和系列划分图解

(a) -TAS 图解(据 Le Maitre, 2002); (b) K_2O - SiO_2 图解(据 Rollinson, 1993); (c) A/NK - A/CNK 图解(据 Maniar and Piccoli, 1989). 安山岩数据来源于赵泽南等(2014); 英云闪长岩数据来源于李文明等(2002), 张连昌等(2004). 图6、图8 数据来源同此图

Fig. 5 Classification and series diagrams of the Tuwu main rocks

(a) -total alkalis vs. silica diagram (Le Maitre, 2002); (b) K_2O vs. SiO_2 diagram (Rollinson, 1993); (c) A/NK vs. A/CNK plot diagram (Maniar and Piccoli, 1989); Data source of andesite from Zhao *et al.* (2014); Data sources of tonalitic rocks from Li *et al.* (2002), Zhang *et al.* (2004). Data sources of andesite and tonalitic rocks in Fig. 6 and Fig. 8 are same as in this figure

为 326Ma。从已有的同位素年代学数据可见,土屋-延东铜矿床成矿年代在 340~320Ma 左右,土屋矿床成矿时代与成岩时代基本一致或稍晚。

4.2 岩石成因

岩石的成因类型和岩浆岩形成的地球动力学过程密切相关,因此对土屋地区英云闪长岩类型的准确判断至关重要。研究表明,埃达克岩是指具有高 Sr、低 Y 等特定地球化学特征的一套中酸性火山岩和侵入岩组合(Kay, 1978)。Defant and Drummond(1990)定义埃达克岩的地球化学特征为: $\text{SiO}_2 > 56\%$, $\text{Al}_2\text{O}_3 > 15\%$, $\text{MgO} < 3\%$, 高 Sr ($> 400 \times 10^{-6}$), 贫 Y 和 Yb ($Y < 18 \times 10^{-6}$, $\text{Yb} < 1.9 \times 10^{-6}$), HREE 明显亏损。本文数据显示土屋英云闪长岩具有与埃达克岩相似的高 Si、Al 和 Sr, 低 Y 和 Yb 的特点。在 Sr/Y-Y 图解和 $(\text{La}/\text{Yb})_N$ - Yb_N 图解中,样品同样落在埃达克岩区域(图8)。因此,土屋英云闪长岩属于埃达克质岩石,其成因模型可以直接用来解释英云闪长岩体的形成。

埃达克岩最初是指产于岛弧环境由年轻洋壳部分熔融形成(Defant and Drummond, 1990)。最近研究表明,埃达克质岩石的成因模型可以包括:(1) 俯冲洋壳的部分熔融(Defant and Drummond, 1990; Rapp *et al.*, 1999; Defant *et al.*, 2002; Martin *et al.*, 2005; 熊小林等, 2005; 王强等, 2006; Zhang *et al.*, 2006; Escuder *et al.*, 2007; Wang *et al.*, 2008, 2013; Zhu *et al.*, 2009b; Tang *et al.*, 2010; Jiang *et al.*, 2012); (2) 增厚下地壳或拆沉下地壳熔融(Atherton and Petford, 1993; Chung *et al.*, 2003; Hou *et al.*, 2004; 熊小林等, 2005; Wen *et al.*, 2008; Huang *et al.*, 2009; He *et al.*, 2011; Guan *et al.*, 2011; 朱志敏等, 2013); (3) 镁铁质岩浆分离结晶作用(Macpherson *et al.*, 2006; Richards and Kerrich, 2007; Richards, 2009, 2011); (4) 地幔岩浆与地壳岩浆的混合作用(Guo *et al.*, 2007, 2009; Streck *et al.*, 2007; Qin *et al.*, 2010; Zhang *et al.*, 2013)等。土屋岩体样品的地球化学特征表明,本区埃达克质岩石最可能来源于俯冲洋壳的部分熔融,证据在于:(1) 相对较高的 MgO 含量

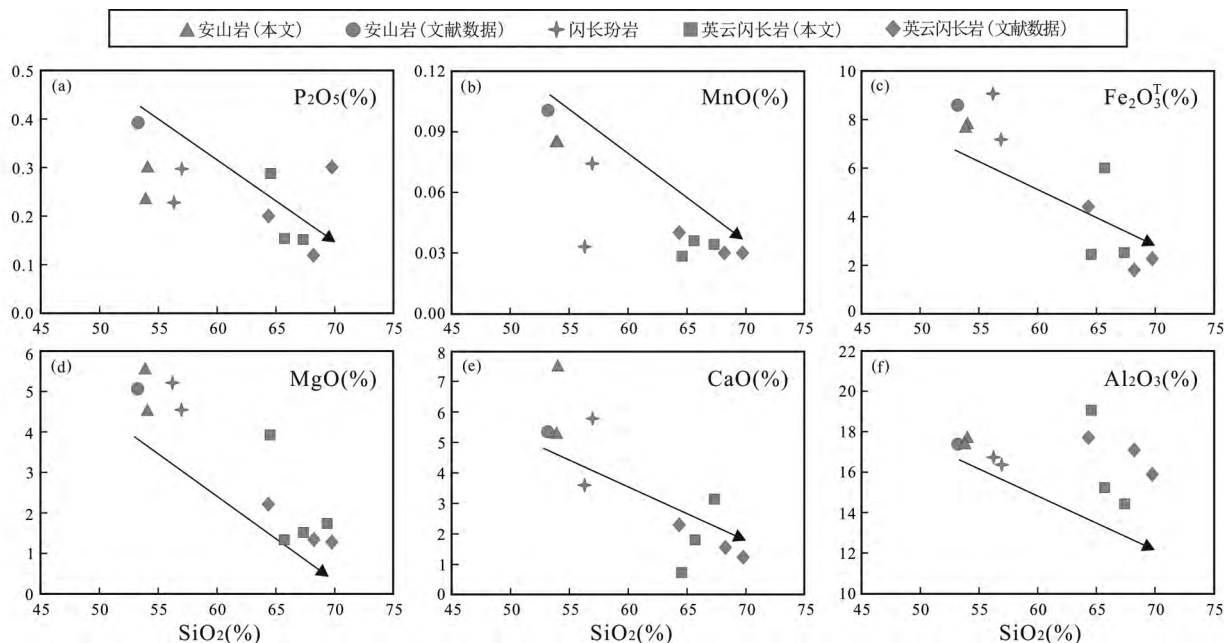


图6 土屋火山岩及英云闪长岩哈克图解

Fig. 6 Harker diagram of the Tuwu volcanic rocks and tonalitic rocks

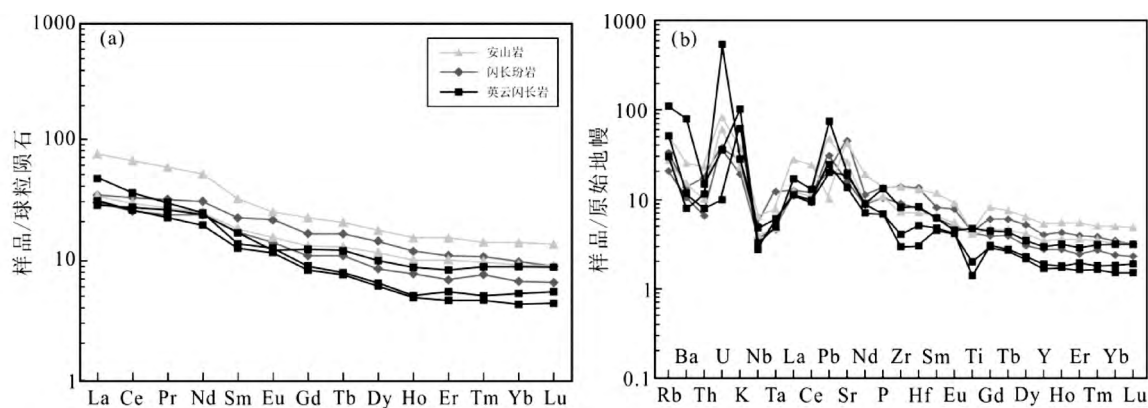


图7 土屋英云闪长岩稀土元素球粒陨石标准化配分图 (a, 标准化值据 Boynton, 1984) 和微量元素原始地幔标准化蛛网图 (b, 标准化值据 Sun and McDonough, 1989)

Fig. 7 Chondrite-normalized REE pattern (a, normalization values after Boynton, 1984) and primitive mantle-normalized trace element abundance spider diagram (b, normalization values after Sun and McDonough, 1989) for the Tuwu tonalitic rocks

(1.28% ~ 3.90%) 或 $Mg^{\#}$ 值 (50 ~ 76), 表明其可能由俯冲洋壳熔融产生, 并经历了与地幔楔橄榄岩的相互作用 (Drummond *et al.*, 1996; Defant *et al.*, 2002); (2) 在 Ce/Yb-Ce 图解中 (图 9), 土屋埃达克质岩石样品投点沿部分熔融线分布, 说明埃达克岩的洋壳熔融成因, 与 Zhang *et al.* (2006) 分析结果一致; (3) 无明显的正 Eu 异常 ($Eu/Eu^* = 0.86 \sim 1.14$) 及锆石 $\varepsilon_{Hf}(t)$ 为正值 (6.3 ~ 16.1), 表明具有与俯冲洋壳相似的特征 (莫宣学等, 2005; Zhu *et al.*, 2009a); (4) 正的 $\varepsilon_{Nd}(t)$ 值 (5.0 ~ 9.4) 和较低的 ($^{87}Sr/^{86}Sr$)_i 值 (0.70316 ~ 0.70378) (芮宗瑶等, 2004; Zhang *et al.*, 2006), 表明其 Sr-Nd 同位素组成接近 MORB 值, 岩浆起源于洋脊玄武质岩石

的部分熔融。由此可见, 土屋英云闪长岩是俯冲玄武质洋壳部分熔融形成的, 埃达克岩熔体形成后与地幔楔橄榄岩发生较弱的交代作用。土屋斑岩铜矿床的赋矿围岩安山岩和闪长玢岩均属于钙碱性系列岩石 (图 5b), 具有相似的微量元素及稀土元素配分模式, 指示二者可能具有同源性。此外, 在 Sr/Y-Y 图解 (图 8a) 和 (La/Yb)_N-Yb_N 图解 (图 8b) 中, 样品均落在岛弧岩石范围内, 表明具有岛弧火山岩的特点, 不同于英云闪长岩的埃达克质特征。

因此, 土屋斑岩型铜矿床英云闪长岩、安山岩及闪长玢岩的地球化学特征表明, 土屋斑岩铜矿床的成矿岩石英云闪长岩具有埃达克质岩石的特征, 而赋矿围岩安山岩及闪长玢

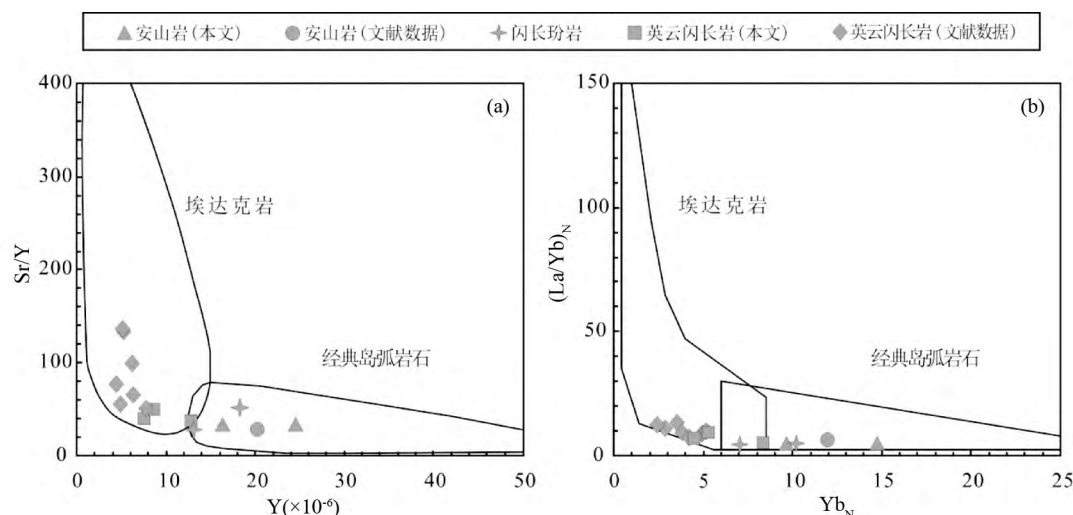


图8 土屋火山岩及英云闪长岩 Sr/Y - Y 图解(a) 和 $(La/Yb)_N$ - Yb_N 图解(b) (据 Defant and Drummond , 1990)

Fig.8 Plots of Sr/Y vs. Y (a) and $(La/Yb)_N$ vs. Yb_N (b) for the Tuwu volcanic rocks and tonalitic rocks (modified after Defant and Drummond , 1990)

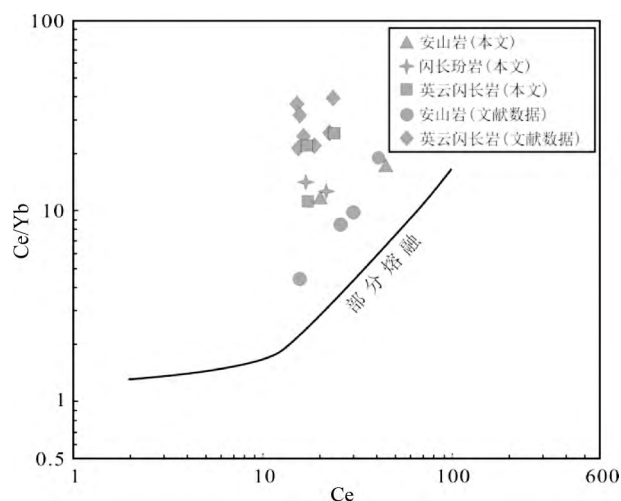


图9 土屋火山岩及英云闪长岩 Ce/Yb - Ce 图解

安山岩数据来源于 Zhang *et al.* (2006) , Shen *et al.* (2014) , 赵泽南等(2014) ; 英云闪长岩岩数据来源同图5

Fig.9 Diagram of Ce/Yb vs. Ce for the Tuwu volcanic rocks and tonalitic rocks

Data sources of andesite from Zhang *et al.* (2006) , Shen *et al.* (2014) , Zhao *et al.* (2014) . Data sources of tonalitic rocks are same as in Fig.5

岩具有同源岛弧火山岩的特点,二者的地球化学特征有显著的差异,指示为不同期岩浆作用的产物。实验岩石学表明,符合埃达克质岩石地球化学特征的岩浆形成压力至少在 1.5 GPa(熊小林等, 2005; 罗照华等, 2010) , 即土屋斑岩型铜矿区深部斑岩体的源区熔融深度可能在 50km 以上。

4.3 地球动力学背景

本文和前人获得的数据均显示,土屋地区岩浆活动大约发生于早石炭世,土屋斑岩铜矿床成矿时代与成岩时代基本一致或稍晚。

新疆北部地区晚古生代构造岩浆活动强烈,经历了板块俯冲、陆-陆碰撞及后碰撞构造演化阶段(王京彬和徐新, 2006; 韩宝福等, 2006; 姜峰和喻亨祥, 2007; Zhou *et al.* , 2008) , 早石炭世至晚二叠世期间的大规模构造岩浆活动,不仅使已经形成的地壳被改造,而且地幔岩浆侵入地壳中,使地壳增厚(李锦轶, 2004) 。根据 MASH 模型(Hildreth and Moor bath, 1998; Hildreth, 2007; Richards, 2003) , 每一个大型弧火山的基线地球化学信号(baseline geochemical signature) 都可以不断被重置,重置过程发生在深部地壳发生重熔和岩浆混合的区域内,因此该区域内存在长时间的幔源岩浆诱捕、贮存和改造过程(Deng *et al.* , 2004, 2007; 罗照华等, 2008, 2010) 。在 Wood(1980) 构造环境判别图解中,新疆土屋矿区火山岩样品均落入岛弧拉斑玄武岩和岛弧钙-碱性玄武岩区(图 10a, b) ; 在 Pearce *et al.* (1984) 构造环境判别图解及 Rb-Hf-Ta 构造图解中,英云闪长岩样品均落入火山弧花岗岩区(图 10c, d) ,表明土屋火山岩及含矿岩体主体均具有岛弧岩浆岩的特点,形成于板块俯冲的构造环境。

早期通常将东天山土屋地区石炭纪岩浆作用解释为: 早泥盆纪准噶尔大洋沿卡拉麦里缝合线的南向俯冲(芮宗瑞等 2002) ; 准噶尔大洋板块在晚古生代向南沿塔里木板块北缘低角度快速俯冲(张连昌等 2004) ; 康古尔塔格大洋板块在石炭世向南北两侧双向俯冲,在康古尔断裂带以北形成大南湖-头苏泉晚古生代岛弧,以南形成阿奇山-雅满苏晚古生代岛弧(王志良等, 2006; Han *et al.* , 2006; 张达玉等,

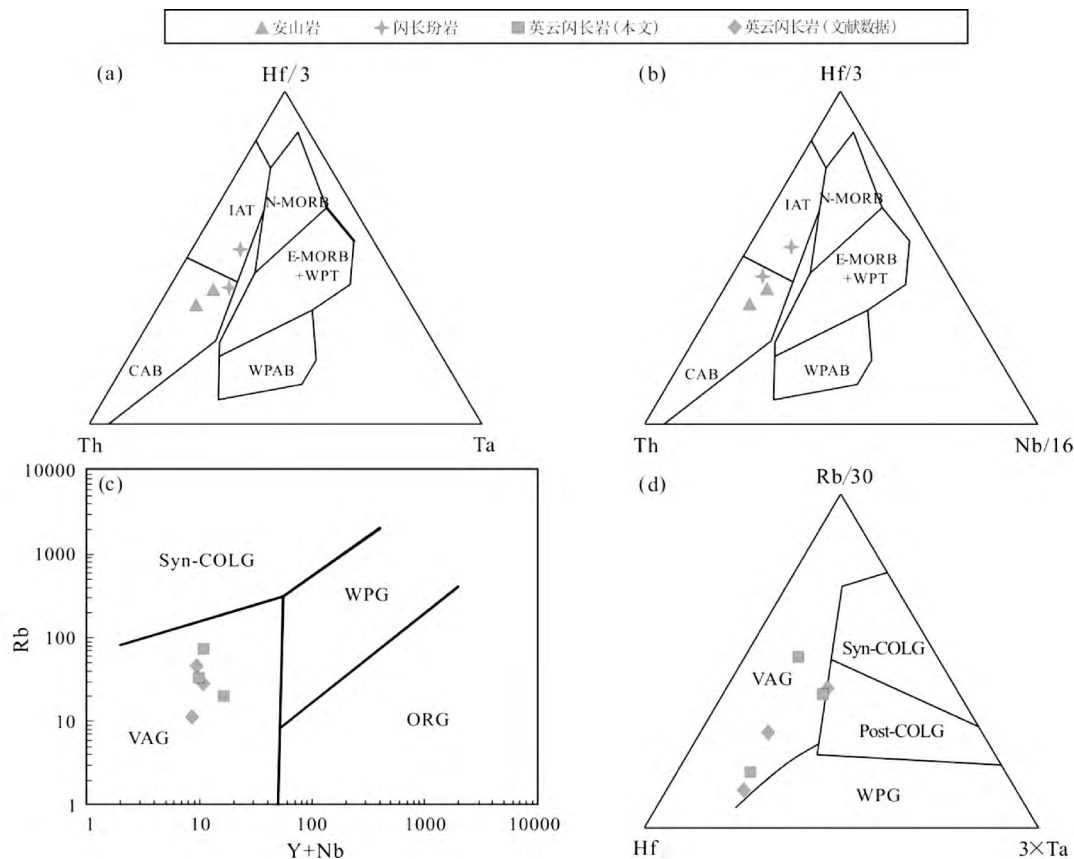


图 10 土屋火山岩及英云闪长岩构造环境判别图解

(a) Hf/3-Th-Ta 图解 (Wood, 1980); (b) Hf/3-Th-Nb/16 图解 (Wood, 1980); (c) Rb-(Y+Nb) 图解 (Pearce *et al.*, 1984); (d) Rb/30-Hf/3-Ta 图解 (Harris *et al.*, 1986). IAT-岛弧拉斑玄武岩; CAB-岛弧钙-碱性玄武岩; WPT-板内拉斑玄武岩; WPAB-板内碱性玄武岩; Syn-COLG-同碰撞花岗岩; VAG-火山弧花岗岩; WPG-板内花岗岩; ORG-洋中脊花岗岩; Post-COLG-碰撞后花岗岩. 英云闪长岩数据来源同图 5

Fig. 10 Tectonic discrimination diagrams for the Tuwu volcanic rocks and tonalitic rocks

(a) Hf/3-Th-Ta diagram (Wood, 1980); (b) Hf/3-Th-Nb/16 diagram (Wood, 1980); (c) Rb-(Y+Nb) diagram (Pearce *et al.*, 1984); (d) Rb/30-Hf/3-Ta diagram (Harris *et al.*, 1986). N-MORB-normal type mid-ocean ridge basalt; E-MORB-enriched MORB; IAT-island arc tholeiite; CAB-calc-alkaline basalts; WPT-within plate tholeiite; WPAB-within plate alkaline tholeiite; Syn-COLG-syn-collision granites; VAG-volcanic arc granites; WPG-within-plate granites; ORG-ocean ridge granites; Post-COLG-post-collision granites. Data sources of tonalitic rocks are same as in Fig. 5

2010)。本文获得的地球化学数据显示,土屋地区英云闪长岩明显富硅,具有亏损 Nb、Ta、Ti、Th 等,富集 K、Rb、Sr、Ba 等地球化学特征,指示其母岩浆形成于与俯冲作用有关的构造环境 (Anderson *et al.*, 1980; Pearce and Peate, 1995)。英云闪长岩具有埃达克质岩石的特征,并且锆石 $\varepsilon_{\text{Hf}}(t)$ 为正值 (+6.3 ~ +16.1),表明其可能来源于俯冲板片的部分熔融。

结合东天山造山带晚古生代区域构造演化特征 (Han and Zhao, 2003; 刘德权等, 2003; Han *et al.*, 2006; 王京彬等, 2006; 顾连兴等, 2006; Zhang *et al.*, 2008; 周涛发等, 2010; Wang *et al.*, 2014b), 本文认为土屋斑岩铜矿床成岩成矿机制为: 早石炭世时期在北天山洋板块北向俯冲的地球动力学背景下,俯冲到深处的大洋板片熔融形成埃达克质岩浆,在熔融过程中同时析出金属,随埃达克质岩浆一起上升,并与地幔橄榄岩发生交代作用,在岩体顶部富集成矿 (图

11)。

5 结论

(1) SIMS 锆石 U-Pb 定年结果表明,土屋地区含矿岩体大约侵位于 335 Ma,土屋斑岩铜矿床成矿时代与成岩时代基本一致或稍晚。

(2) 地球化学数据显示,土屋斑岩铜矿床中的安山岩、闪长玢岩及英云闪长岩样品均富集 K、Rb、Sr、Ba 等大离子亲石元素,相对亏损 Nb、Ta、Ti、Th 等高场强元素,安山岩和闪长玢岩具有同源性及岛弧火山岩的特点,英云闪长岩具有埃达克质岩石的特征。土屋英云闪长岩具不均一的锆石 $\varepsilon_{\text{Hf}}(t)$ 正值 (+6.3 ~ +16.1),表明其可能来源于俯冲板片的部分熔融。

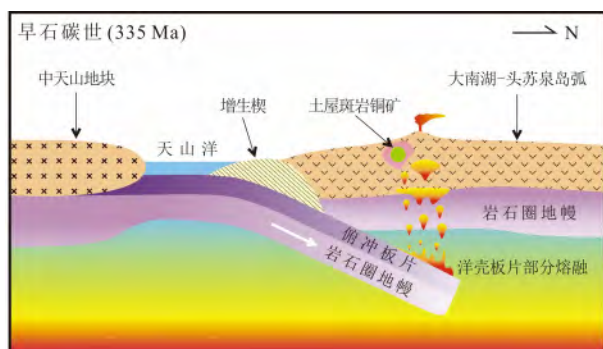


图 11 东天山地球动力学背景模式图

Fig. 11 Schematic diagram showing the geodynamic setting in the eastern Tianshan

(3) 土屋斑岩铜矿床含矿岩体是早石炭世时期在北天山洋板块北向俯冲的地球动力学背景下, 俯冲到深处的大洋板片熔融形成埃达克质岩浆, 在熔融过程中同时析出金属, 随埃达克质岩浆一起上升, 并与地幔橄榄岩发生交代作用, 在岩体顶部富集成矿。

致谢 野外工作中得到了新疆地质矿产开发局董连慧总工程师和中亚黄金集团陈昌龙副总裁的大力支持和帮助; 室内研究中得到了中国地质大学(北京) 翟裕生院士、罗照华教授、朱弟成教授和苏犁教授的关心和帮助; 论文评审中评审专家对论文初稿提出了宝贵的修改意见; 谨致谢忱。

References

- Anderson RN, Delong SE and Schwarz WM. 1980. Dehydration, asthenospheric convection and seismicity in subduction zones. *The Journal of Geology*, 88(4): 445–451
- Atherton MP and Petford N. 1993. Generation of sodium-rich magmas from newly underplated basaltic crust. *Nature*, 362(6416): 144–146
- Boynton WV. 1984. Geochemistry of the rare earth elements: Meteorite studies. In: Henderson P (ed.). *Rare Earth Element Geochemistry*. Amsterdam: Elsevier
- Chen FW, Li HQ, Chen YC, Wang DH, Wang JL, Liu DQ, Tang YL and Zhou RH. 2005. Zircon SHRIMP U-Pb dating and its geological significance of mineralization in Tuwu-Yandong porphyry copper mine, East Tianshan Mountain. *Acta Geologica Sinica*, 79(2): 247–254 (in Chinese with English abstract)
- Chen W, Sun S, Zhang Y, Xiao WJ, Wang YT, Wang QL, Jiang LF and Yang JT. 2005. $^{40}\text{Ar}/^{39}\text{Ar}$ geochronology of the Qiugemingtashi-Huangshan ductile shear zone in East Tianshan, Xinjiang, NW China. *Acta Geologica Sinica*, 79(6): 790–804 (in Chinese with English abstract)
- Chen YJ, Chen HY, Zaw K, Pirajno F and Zhang ZJ. 2007. Geodynamic settings and tectonic model of skarn gold deposits in China: An overview. *Ore Geology Reviews*, 31(1–4): 139–169
- Chen YJ, Pirajno F, Wu G, Qi JP and Xiong XL. 2012. Epithermal deposits in North Xinjiang, NW China. *International Journal of Earth Sciences*, 101(4): 889–917
- Chung SL, Liu DY, Ji JQ, Chu MF, Lee HY, Wen DJ, Lo CH, Lee TY, Qian Q and Zhang Q. 2003. Adakites from continental collision zones: Melting of thickened lower crust beneath southern Tibet.

- Geology*, 31(11): 1021–1024
- Defant MJ and Drummond MS. 1990. Derivation of some modern arc magmas by melting of young subducted lithosphere. *Nature*, 347(6294): 662–665
- Defant MJ, Xu JF, Kepezhinskas P, Wang Q, Zhang Q and Xiao L. 2002. Adakites: Some variations on a theme. *Acta Petrologica Sinica*, 18(2): 129–142
- Deng J, Wang QF, Xiao CH, Yang LQ, Liu H and Gong QJ. 2011. Tectonic-magmatic-metallogenic system, Tongling ore cluster region, Anhui Province, China. *International Geology Review*, 53(5–6): 449–476
- Deng J, Wang QF, Li GJ, Li CS and Wang CM. 2013. Tethys tectonic evolution and its bearing on the distribution of important mineral deposits in the Sanjiang region, SW China. *Gondwana Research*, 26(2): 419–437
- Deng J, Wang QF, Li GJ and Santosh M. 2014. Cenozoic tectono-magmatic and metallogenic processes in the Sanjiang region, southwestern China. *Earth Science Reviews*, 138: 268–299
- Deng JF, Mo XX, Luo ZH, Wang Y, Zhao HL, Zhao ZD, Su SG and Yu XH. 2001. Inhomogeneity of the lithosphere of the Tibetan Plateau and implications for geodynamics. *Science in China (Series D)*, 44(S1): 56–63
- Deng JF, Mo XX, Zhao HL, Wu ZX, Luo ZH and Su SG. 2004. A new model for the dynamic evolution of Chinese lithosphere: Continental roots-plume tectonics. *Earth-Science Reviews*, 65(3–4): 223–275
- Deng JF, Su SG, Niu YL, Liu C, Zhao GC, Zhao XG, Zhou S and Wu ZX. 2007. A possible model for the lithospheric thinning of North China Craton: Evidence from the Yanshanian (Jura-Cretaceous) magmatism and tectonism. *Lithos*, 96(1–2): 22–35
- Drummond MS, Defant MJ and Kepezhinskas PK. 1996. Petrogenesis of slab-derived trondhjemite-tonalite-dacite/adakite magmas. *Transactions of the Royal Society of Edinburgh: Earth Sciences*, 87(1–2): 205–215
- Escuder VJ, Contreras F, Stein G, Urien P, Joubert M, Pérez-Estaún A, Friedman R and Ullrich T. 2007. Magmatic relationships and ages between adakites, magnesian andesites and Nb-enriched basalt-andesites from Hispaniola: Record of a major change in the Caribbean island arc magmasources. *Lithos*, 99(3–4): 151–177
- Gu LX, Zhang ZZ, Wu CZ, Wang YX, Tang JH, Wang CS, Xi AH and Zheng YC. 2006. Some problems on granites and vertical growth of the continental crust in the eastern Tianshan Mountains, NW China. *Acta Petrologica Sinica*, 22(5): 1103–1120 (in Chinese with English abstract)
- Guan Q, Zhu DC, Zhao ZD, Dong GC, Zhang LL, Li XW, Liu M, Mo XX, Liu YS and Yuan HL. 2011. Crustal thickening prior to 38Ma in southern Tibet: Evidence from lower crust-derived adakitic magmatism in the Gangdese Batholith. *Gondwana Research*, 21(1): 88–89
- Guo F, Nakamura E, Fan WM, Kobayoshi K and Li CW. 2007. Generation of Palaeocene adakitic andesites by magma mixing, Yanji area, NE China. *Journal of Petrology*, 48(4): 661–692
- Guo F, Nakamura E, Fan WM, Kobayoshi K, Li CW and Gao XF. 2009. Mineralogical and geochemical constraints on magmatic evolution of Paleocene adakitic andesites from the Yanji area, NE China. *Lithos*, 112(3–4): 321–341
- Guo QQ, Pan CZ, Xiao WJ, Qu JF, Ao SJ, Zhang JE, Song DF, Tian ZH, Wan B and Han CM. 2010. Geological and geochemical characteristics of the Yandong porphyry copper deposits in Hami, Xinjiang. *Xinjiang Geology*, 28(4): 419–426 (in Chinese with English abstract)
- Han BF, Ji JQ, Song B, Chen LH and Zhang L. 2006. Late Paleozoic vertical growth of continental crust around the Junggar Basin, Xinjiang, China (Part I): Timing of post-collisional plutonism. *Acta Petrologica Sinica*, 22(5): 1077–1086 (in Chinese with English abstract)
- Han CM and Zhao GC. 2003. Major types and characteristics of Late Paleozoic ore deposits, East Tianshan, Northwest China.

- International Geology Review, 45(9): 798–813
- Han CM, Xiao WJ, Zhao GC, Mao JW, Li SZ, Yan Z and Mao QG. 2006. Major types, characteristics and geodynamic mechanism of Upper Paleozoic copper deposits in northern Xinjiang, northwestern China. *Ore Geology Reviews*, 28(3): 308–328
- Harris HBW, Pearce JA and Tindle AG. 1986. Geochemical characteristics of collision-zone magmatism. *Geological Society London, Special Publications*, 19(1): 67–81
- He YS, Li SG, Hoefs J, Huang F, Liu SA and Hou ZH. 2011. Post-collisional granitoids from the Dabie orogen: New evidence for partial melting of a thickened continental crust. *Geochimica et Cosmochimica Acta*, 75(13): 3815–3838
- Hildreth W and Moorbath S. 1988. Crustal contributions to arc magmatism in the Andes of central Chile. *Contributions to Mineralogy and Petrology*, 98(4): 455–489
- Hildreth W. 2007. Quaternary magmatism in the Cascades: Geological perspectives. *USGS Professional Paper*, 1744: 1–125
- Hoefs J. 1997. *Stable Isotope Geochemistry*. 3rd Edition. Berlin: Springer Verlag, 1–250
- Hoskin PWO and Schaltegger U. 2003. The composition of zircon and igneous and metamorphic petrogenesis. *Reviews of Mineralogy and Geochemistry*, 53(1): 27–62
- Hou GS and Yang HJ. 2009. The petrogenesis of Tuwu plagiogranite porphyry from East Tianshan: Evidence from wallrock. *Sichuan Nonferrous Metals*, (2): 5–8 (in Chinese with English abstract)
- Hou KJ, Li YH, Zou TR, Qu XM, Shi YR and Xie GQ. 2007. Laser ablation-MC-ICP-MS technique for Hf isotope microanalysis of zircon and its geological applications. *Acta Petrologica Sinica*, 23(10): 2595–2604 (in Chinese with English abstract)
- Hou ZQ, Gao YF, Qu XM, Rui ZY and Mo XX. 2004. Origin of adakitic intrusives generated during Mid-Miocene east-west extension in southern Tibet. *Earth and Planetary Science Letters*, 220(1–2): 139–155
- Huang XL, Xu YG, Lan JB, Yang QJ and Luo ZY. 2009. Neoproterozoic adakitic rocks from Mopanshan in the western Yangtze Craton: Partial melts of thickened lower crust. *Lithos*, 112(3–4): 367–381
- Jiang ZQ, Wang Q, Li ZX, Wyman DA, Tang GJ, Jia XH and Yang YH. 2012. Late Cretaceous (ca. 90Ma) adakitic intrusive rocks in the Kelu area, Gangdese Belt (southern Tibet): Slab melting and implications for Cu–Au mineralization. *Journal of Asian Earth Sciences*, 53: 67–81
- Kay RW. 1978. Aleutian magnesian andesites: Melts from subducted Pacific Ocean crust. *Journal of Volcanology and Geothermal Research*, 4(1–2): 117–132
- Le Maitre RW. 2002. *Igneous Rocks: A Classification and Glossary of Terms*. 2nd Edition. Cambridge: Cambridge University Press, 33–39
- Li HQ, Xie CF and Chang HL. 1998. Study on Metallogenetic Chronology of Nonferrous and Precious Metallic Ore Deposits in Northern Xinjiang, China. Beijing: Geological Publishing House, 1–267 (in Chinese with English abstract)
- Li JY. 2004. Late Neoproterozoic and Paleozoic tectonic framework and evolution of eastern Xinjiang, NW China. *Geological Review*, 50(3): 304–322 (in Chinese with English abstract)
- Li WM, Ren BC, Yang XK, Li YZ and Chen Q. 2002. The intermediate-acid intrusive magmatism and its geodynamic significance in eastern Tianshan region. *Northwestern Geology*, 35(4): 41–64 (in Chinese with English abstract)
- Li XH, Liu Y, Li QL, Guo CH and Chamberlain KR. 2009. Precise determination of Phanerozoic zircon Pb/Pb age by multi-collector SIMS without external standardization. *Geochimica et Geophysica*, 10(4): 1–21
- Li YP, Sun GH, Li JY, Wang YB, Xu X, He GQ and Jia JD. 2006. Devonian granite on the eastern margin of the Tuha basin in the East Tianshan, Xinjiang, China and its tectonic implication. *Geological Bulletin of China*, 25(8): 932–936 (in Chinese with English abstract)
- Li ZM, Zhao RF, Huo RP and Wang QM. 2006. Geological characters of Tuwu–Yandong copper deposit in Xinjiang. *Geology and Prospecting*, 42(6): 1–4 (in Chinese with English abstract)
- Liu DQ, Chen YC, Wang DH, Tang YL, Zhou RH, Wang JL, Li HQ and Chen FW. 2003. A discussion on problems related to mineralization of Tuwu–Yandong Cu–Mo orefield in Hami. *Xinjiang Mineral Deposits*, 22(4): 334–344 (in Chinese with English abstract)
- Liu M, Zhu DC, Zhao ZD, Wang LQ, Mo XX and Zhou CY. 2009. Early Cretaceous magma mixing in Ranwu area of eastern Gangdese, Tibet: Evidence from zircon SHRIMP U–Pb age and Hf isotopic composition. *Earth Science Frontiers*, 16(2): 1446–1455 (in Chinese with English abstract)
- Liu XM. 2000. Tectonic settings and characteristics of post-collisional magmatic rocks. *Progress in Precambrian Research*, 23(2): 121–127 (in Chinese with English abstract)
- Lou F and Yu HX. 2007. Tectonic characteristics of post-collision in north of Xinjiang. *China Science and Technology Information*, (22): 19–20 (in Chinese with English abstract)
- Ludwig KR. 2001. *Users Manual for Isoplot /Ex rev. 2.49: A geochronological Toolkit for Microsoft Excel*. Berkeley Geochronology Centre Special Publication
- Luo ZH, Mo XX, Lu XX, Chen BH, Ke S, Hou ZQ and Jiang W. 2007. Metallogeny by trans-magmatic fluids-theoretical analysis and field evidence. *Earth Science Frontiers*, 14(3): 165–183 (in Chinese with English abstract)
- Luo ZH, Lu XX, Chen BH, Huang F, Yang ZF and Wang BZ. 2008. The constraints from deep processes on the porphyry metallogenesis in collisional orogens. *Acta Petrologica Sinica*, 24(3): 447–456 (in Chinese with English abstract)
- Luo ZH, Lu XX, Xu JY, Liu C and Li DD. 2010. Petrographic indicators of the ore-bearing intrusions. *Acta Petrologica Sinica*, 26(8): 2247–2254 (in Chinese with English abstract)
- Luo ZH. 2012. The theory of metallogeny by the small magmatic intrusion: Meaning and implications. *Northwestern Geology*, 45(4): 204–215 (in Chinese with English abstract)
- Macpherson CG, Dreher ST and Thirlwall MF. 2006. Adakites without slab melting: High pressure differentiation of island arc magma, Mindanao, the Philippines. *Earth and Planetary Science Letters*, 243(3–4): 581–593
- Maniar PD and Piccoli PM. 1989. Tectonic discrimination of granitoids. *Geological Society of America Bulletin*, 101(5): 635–643
- Martin H, Smithies RH, Rapp R, Moyen JF and Champion D. 2005. An overview of adakite, tonalite-trondhjemite-granodiorite (TTG), and sanukitoid: Relationship and some implications for crustal evolution. *Lithos*, 79(1–2): 1–24
- Mo XX, Dong GC, Zhao ZD, Zhou S, Wang LL, Qiu RZ and Zhang FQ. 2005. Spatial and temporal distribution and characteristics of granitoids in the Gangdese, Tibet and implication for crustal growth and evolution. *Geological Journal of China Universities*, 11(3): 281–290 (in Chinese with English abstract)
- Morel MLA, Nebel O, Nebel-Jacobsen YJ, Miller JS and Vroon PZ. 2008. Hafnium isotope characterization of the GJ-1 zircon reference material by solution and laser-ablation MC-ICPMS. *Chemical Geology*, 255(1–2): 231–235
- Pan HD, Shen P, Chen G, Yang JT, Zhao YJ and Dai HW. 2013. Volcanic-plutonic complex, ore-forming rocks and their alterations in Tuwu porphyry Cu deposit of Xinjiang. *Mineral Deposits*, 32(4): 794–808 (in Chinese with English abstract)
- Pearce JA, Harris NBW and Tindle AC. 1984. Trace element discrimination diagrams for the tectonic interpretation of granitic rocks. *Journal of Petrology*, 25(4): 956–983
- Pearce JA and Peate DW. 1995. Tectonic implications of the compositions of volcanic arc magmas. *Annual Reviews in Earth and Planetary Sciences*, 23: 252–285
- Pirajno F. 2009. *Hydrothermal Processes and Mineral Systems*. Berlin: Springer, 1–1250
- Pirajno F. 2013. *The Geology and Tectonic Settings of China's Mineral*

- Deposits. Berlin: Springer, 1-671
- Qin JF, Lai SC, Diwu CR, Ju YJ and Li YF. 2010. Magma mixing origin for the post-collisional adakitic monzogranite of the Triassic Yangba pluton, Northwestern margin of the South China block: Geochemistry, Sr-Nd isotopic, zircon U-Pb dating and Hf isotopic evidences. *Contributions to Mineralogy and Petrology*, 159(3): 389-409
- Qin KZ. 2000. Metellogenesis in relation to Central-Asia Style orogeny of northern Xinjiang. Post-Doctor Research Report. Beijing: Institute of Geology and Geophysics, Chinese Academy of Sciences, 71-157 (in Chinese with English summary)
- Qin KZ, Fang TH, Wang SL, Zhu BQ, Feng YM, Yu HF and Xiu QY. 2002. Plate tectonics division, evolution and metallogenic settings in eastern Tianshan Mountains, NW China. *Xinjiang Geology*, 20(4): 302-308 (in Chinese with English abstract)
- Qin KZ, Su BX, Sakyi PA, Tang DM, Li XH, Sun H, Xiao QH and Liu PP. 2011. SIMS zircon U-Pb geochronology and Sr-Nd isotopes of Ni-Cu bearing mafic-ultramafic intrusions in eastern Tianshan and Beishan in correlation with flood basalts in Tarim basin (NW China): Constraints on a ca. 280Ma mantle plume. *American Journal of Science*, 311(3): 237-260
- Rapp PR, Shimizu N, Norman MD and Applegate GS. 1999. Reaction between slab-derived melt and peridotite in the mantle wedge: Experimental constraints at 3.8GPa. *Chemical Geology*, 160(4): 335-356
- Richards JP. 2003. Tectono-magmatic precursors for porphyry Cu-(Mo-Au) deposit formation. *Economic Geology*, 98(8): 1515-1533
- Richards JP and Kerrich R. 2007. Special paper: Adakite-like rocks: Their diverse origins and questionable role in metallogenesis. *Economic Geology*, 102(4): 537-576
- Richards JP. 2009. Postsubduction porphyry Cu-Au and epithermal Au deposits: Products of remelting of subduction-modified lithosphere. *Geology*, 37(3): 247-250
- Richards JP. 2011. High Sr/Y arc magmas and porphyry Cu \pm Mo \pm Au deposits: Just add water. *Economic Geology*, 106(7): 1075-1081
- Rollinson HR. 1993. Using Geochemical Data: Evaluation, Presentation, Interpretation. New York: Longman Group UK Ltd., 1-352
- Rui ZY, Liu YL, Wang LS and Wang YT. 2002. The eastern Tianshan porphyry copper belt in Xinjiang and its tectonic framework. *Acta Geologica Sinica*, 76(1): 83-94 (in Chinese with English abstract)
- Rui ZY, Zhang LS, Chen ZY, Wang LS, Liu YL and Wang YT. 2004. Approach on source rock or source region of porphyry copper deposit. *Acta Petrologica Sinica*, 20(2): 229-238 (in Chinese with English abstract)
- Shen P, Pan HD, Dong LH, Yang JS, Shen YC, Dai HW, Guan WN and Zhao YJ. 2012. Caldera complex, hosted rocks and alteration of the Yandong porphyry copper deposit in eastern Tianshan, Xinjiang. *Acta Petrologica Sinica*, 28(7): 1966-1980 (in Chinese with English abstract)
- Shen P, Pan HD, Dong LH and Li XH. 2014. Yandong porphyry Cu deposit, Xinjiang, China: Geology, geochemistry and SIMS U-Pb zircon geochronology of host porphyries and associated alteration and mineralization. *Journal of Asian Earth Sciences*, 80: 197-217
- Soderlund U, Patchett PJ, Vervoort JD and Isachsen CE. 2004. The ^{176}Lu decay constant determined by Lu-Hf and U-Pb isotope systematics of Precambrian mafic intrusions. *Earth and Planetary Science Letters*, 219(3-4): 311-324
- Stacey JS and Kramers JD. 1975. Approximation of terrestrial lead isotope evolution by a two-stage model. *Earth and Planetary Science Letters*, 26(2): 207-221
- Streck MJ, Leeman PW and Chesley J. 2007. High-magnesian andesite from Mount Shasta: A product of magma mixing and contamination, not a primitive mantle melt. *Geology*, 35(4): 351-354
- Sun SS and McDonough WF. 1989. Chemical and isotope systematics of oceanic basalts: Implications for mantle composition and processes. In: Saunders AD and Norry MJ (eds.). *Magmatism in Ocean Basins*. London: Geological Society Special Publication, 42(1): 313-345
- Sylvester PJ. 1998. Post-collisional strongly peraluminous granites. *Lithos*, 45(1-4): 29-44
- Tang GJ, Wang Q, Wyman DA, Li ZX, Zhao ZH, Jia XH and Jiang ZQ. 2010. Ridge subduction and crustal growth in the Central Asian Orogenic Belt: Evidence from Late Carboniferous adakites and high-Mg diorites in the western Junggar region, northern Xinjiang (West China). *Chemical Geology*, 277(3-4): 281-300
- Tang JH, Gu LX, Zhang ZZ, Wu CZ, San JZ, Wang CS, Liu SH and Zhang GH. 2007. Characteristics age and origin of the Xianshuiquan gneissose granite in eastern Tianshan. *Acta Petrologica Sinica*, 23(8): 1803-1820 (in Chinese with English abstract)
- Wang BQ, Zhou MF, Li JW and Yan DP. 2013. Late Triassic porphyritic intrusions and associated volcanic rocks from the Shangri-La region, Yidun terrane, eastern Tibetan Plateau: Adakitic magmatism and porphyry copper mineralization. *Lithos*, 127(1-2): 24-38
- Wang FT, Feng J, Hu JW, Wang L, Jiang LF and Zhang Z. 2001. Characteristics and significance of the Tuwu porphyry copper deposit, Xinjiang. *Geology in China*, 28(1): 36-39 (in Chinese with English abstract)
- Wang JB and Xu X. 2006. Post-collisional tectonic evolution and metallogenesis in northern Xinjiang, China. *Acta Geologica Sinica*, 80(1): 23-31 (in Chinese with English abstract)
- Wang JB, Wang YW and He ZJ. 2006. Ore deposits as a guide to the tectonic evolution in the East Tianshan Mountains, NW China. *Geology in China*, 33(3): 461-469 (in Chinese with English abstract)
- Wang LS, Li HQ, Liu DQ and Chen YC. 2005. Geological characteristics and mineralization epoch of Weiquan silver (copper) deposit, Hami, Xinjiang, China. *Mineral Deposits*, 22(3): 280-284 (in Chinese with English abstract)
- Wang Q, Zhao ZH, Xu JF, Wyman DA, Xiong XL, Zi F and Bai ZH. 2006. Carboniferous adakite-high-Mg andesite-Nb-enriched basaltic rock suites in the northern Tianshan area: Implications for Phanerozoic crustal growth in the Central Asia Orogenic Belt and Cu-Au mineralization. *Acta Petrologica Sinica*, 22(1): 11-30 (in Chinese with English abstract)
- Wang Q, Wyman DA, Xu JF, Wan YS, Li CF, Zi F, Jiang ZQ, Qiu HN, Chu ZY, Zhao ZH and Dong YH. 2008. Triassic Nb-enriched basalts, magnesian andesites, and adakites of the Qiangtang terrane (Central Tibet): Evidence for metasomatism by slab-derived melts in the mantle wedge. *Contributions to Mineralogy and Petrology*, 155(4): 473-490
- Wang T, Jahn BM, Victor P, Kovach, Tong Ys, Hong DW and Han BF. 2009. Nd-Sr isotopic mapping of the Chinese Altai and implications for continental growth in the Central Asian Orogenic Belt. *Lithos*, 110(1-4): 359-372
- Wang YH, Xue CJ, Wang JP, Peng RM, Yang JT, Zhang FF, Zhao ZN and Zhao YJ. 2014a. Petrogenesis of magmatism in the Yandong region of eastern Tianshan, Xinjiang: Geochemical, geochronological and Hf isotope constraints. *International Geology Review*, doi: 10.1080/00206814.2014.900653
- Wang YH, Xue CJ, Liu JJ, Wang JP, Yang JT, Zhang FF, Zhao ZN, Zhao YJ and Liu B. 2014b. Early Carboniferous adakitic rocks in the area of the Tuwu deposit, eastern Tianshan, NW China: Slab melting and implications for porphyry copper mineralization. *Journal of Asian Earth Sciences*, doi: 10.1016/j.jseaes.2014.09.032
- Wang ZL, Mao JW, Zhang ZH, Zuo GC and Wang LS. 2006. Geology, time-space distribution and metallogenic geodynamic evolution of porphyry copper (molybdenum) deposits in the Tianshan Mountains. *Acta Geologica Sinica*, 80(7): 943-955 (in Chinese with English abstract)
- Wen DR, Chung SL, Song B, Iizuka Y, Yang HJ, Ji JQ, Liu DY and Gallet S. 2008. Late Cretaceous Gangdese intrusions of adakitic geochemical characteristics, SE Tibet: Petrogenesis and tectonic implications. *Lithos*, 105(1-2): 1-11
- Wood DA. 1980. The application of a Th-Hf-Ta diagram to problems of

- tectonomagmatic classification and to establishing the nature of crustal contamination of basaltic lavas of the British Tertiary volcanic province. *Earth and Planetary Science Letters*, 50(1): 11–30
- Wu CZ, Zhang ZZ, Khin Z, Fernando DP, Tang JH, Zheng YC, Wang CS and San JZ. 2006. Geochronology, geochemistry and tectonic significances of the Hongyuntan granitoids in the Qoltag area, eastern Tianshan. *Acta Petrologica Sinica*, 22(5): 1121–1134 (in Chinese with English abstract)
- Wu ZN, Huang JH, Yusufuaili QR, Muhtar Z, Yiang XR, Dilixiati and Han WQ. 2007. Certain geochemical characteristics for copper metallogenesis in Tuwu, Xinjiang. *Xinjiang Geology*, 25(2): 160–163 (in Chinese with English abstract)
- Xiong XL, Cai ZY, Niu HC, Chen YB, Wang Q, Zhao ZH and Wu JH. 2005. The Late Paleozoic adakites in eastern Tianshan area and their metallogenetic significance. *Acta Petrologica Sinica*, 21(3): 967–976 (in Chinese with English abstract)
- Yuan WM, Bao ZK, Dong JQ, Guo ZJ and Deng J. 2007. Zircon and apatite fission track analyses on mineralization ages and tectonic activities of Tuwu-Yandong porphyry copper deposit in northern Xinjiang, China. *Science in China (Series D)*, 50(12): 1787–1795
- Zhai YS, Wang JP, Peng RM and Liu JJ. 2009. Research on superimposed metallogenic systems and polygenetic mineral deposits. *Earth Science Frontiers*, 16(6): 282–290 (in Chinese with English abstract)
- Zhai YS, Yao SZ and Cai KQ. 2011. *Mineral Deposits*. 3rd Edition. Beijing: Geological Publishing House (in Chinese)
- Zhang C, Ma C, Holtz F, Koepke J, Wolff PF and Berndt J. 2013. Mineralogical and geochemical constraints on contribution of magma mixing and fractional crystallization to high-Mg adakite-like diorites in eastern Dabie orogen, East China. *Lithos*, 172–173: 118–138
- Zhang DY, Zhou TF, Yuan F, Fan Y, Liu S and Peng MX. 2010. Geochemical characters, metallogenic chronology and geological significance of the Yanxi copper deposit in eastern Tianshan, Xinjiang. *Acta Petrologica Sinica*, 26(11): 3327–3338 (in Chinese with English abstract)
- Zhang LC, Qin KZ, Ying JF, Xia B and Shu JS. 2004. The relationship between ore-forming processes and adakitic rock in Tuwu-Yandong porphyry copper metallogenic belt, eastern Tianshan Mountains. *Acta Petrologica Sinica*, 20(2): 259–268 (in Chinese with English abstract)
- Zhang LC, Xiao WJ, Qin KZ and Zhang Q. 2006. The adakite connection of the Tuwu-Yandong copper porphyry belt, eastern Tianshan, NW China: Trace element and Sr-Nd-Pb isotope geochemistry. *Mineralium Deposita*, 41(2): 188–200
- Zhang LC, Qin KZ and Xiao WJ. 2008. Multiple mineralization events in the eastern Tianshan district, NW China: Isotopic geochronology and geological significance. *Journal of Asian Earth Sciences*, 32(2–4): 236–246
- Zhang ZZ, Gu LX, Wu CZ, Li WQ, Xi AH and Wang S. 2005. Zircon SHRIMP dating for the Weiya pluton, eastern Tianshan: Its geological implications. *Acta Geologica Sinica*, 79(4): 481–490
- Zhao ZN, Wang YH, Wang JP, Dong LS, Zhang FF and Liu B. 2014. Geochemistry of volcanic rocks of Qi'eshan group in the Tuwu copper deposit and its geological significance. *Journal of Mineralogy and Petrology*, 34(1): 63–69 (in Chinese with English abstract)
- Zhou TF, Yuan F, Fan Y, Zhang DY, David C and Zhao GC. 2008. Granites in the Sawuer region of the West Junggar, Xinjiang Province, China: Geochronological and geochemical characteristics and their geodynamic significance. *Lithos*, 106(3–4): 191–206
- Zhou TF, Yuan F, Zhang DY, Fan Y, Liu S, Peng MX and Zhang JD. 2010. Geochronology, tectonic setting and mineralization of granitoids in Jueluotage area, eastern Tianshan, Xinjiang. *Acta Petrologica Sinica*, 26(2): 478–502 (in Chinese with English abstract)
- Zhu DC, Mo XX, Wang LQ, Zhao ZD, Niu YL, Zhou CY and Yang YH. 2009a. Petrogenesis of highly fractionated I-type granites in the Zayu area of eastern Gangdese, Tibet: Constraints from zircon U-Pb geochronology, geochemistry and Sr-Nd-Hf isotopes. *Science in China (Series D)*, 52(9): 1223–1239
- Zhu DC, Pan GT, Zhao ZD, Lee HY, Kang ZQ, Liao ZL, Wang LQ, Li GM, Dong GC and Liu B. 2009b. Early Cretaceous subduction-related adakite-like rocks in the Gangdese belt, South Tibet: Products of slab melting and subsequent melt-peridotite interaction? *Journal of Asian Earth Sciences*, 34(3): 298–309
- Zhu ZM, Xiong XL, Chu FY and Wu YH. 2013. Geochemistry and petrogenesis of core samples from Baishan molybdenum deposit, East Tianshan Mountains, Xinjiang. *Acta Petrologica Sinica*, 29(1): 167–177 (in Chinese with English abstract)

附中文参考文献

- 陈富文, 李华芹, 陈毓川, 王登红, 王金良, 刘德权, 唐延龄, 周汝洪. 2005. 东天山土屋-延东斑岩铜矿田成岩时代精确测定及其地质意义. *地质学报*, 79(2): 247–254
- 陈文, 孙枢, 张彦, 肖文交, 王义天, 王清利, 姜立丰, 杨俊强. 2005. 新疆东天山秋格明塔什-黄山韧性剪切带⁴⁰Ar/³⁹Ar年代学研究. *地质学报*, 79(6): 790–804
- 顾连兴, 张遵忠, 吴昌志, 王银喜, 唐俊华, 汪传胜, 郑爱华, 郑远川. 2006. 关于东天山花岗岩与陆壳垂向增生的若干认识. *岩石学报*, 22(5): 1103–1122
- 郭谦谦, 潘成泽, 肖文交, 曲军峰, 敖松坚, 张继恩, 宋东方, 田中华, 万博, 韩春明. 2010. 哈密延东铜矿床地质和地球化学特征. *新疆地质*, 28(4): 419–426
- 韩宝福, 季建清, 宋彪, 陈立辉, 张磊. 2006. 新疆准噶尔晚古生代陆壳垂向生长(I)——后碰撞深成岩浆活动的时限. *岩石学报*, 22(5): 1077–1086
- 侯广顺, 杨贺杰. 2009. 东天山土屋斜长花岗斑岩的成因——来自围岩的证据. *四川有色金属*, (2): 5–8
- 侯可军, 李延河, 邹天人, 曲晓明, 石玉若, 谢桂青. 2007. LA-MC-ICP-MS 锆石 Hf 同位素的分析方法及地质应用. *岩石学报*, 23(10): 2595–2604
- 李华芹, 谢才富, 常海亮. 1998. 新疆北部有色贵金属矿床成矿作用年代学. 北京: 地质出版社, 1–267
- 李锦轶. 2004. 新疆东部新元古代晚期和古生代构造格局及其演变. *地质论评*, 50(3): 304–322
- 李文明, 任秉琛, 杨兴科, 李有柱, 陈强. 2002. 东天山中酸性侵入岩浆作用及其地球动力学意义. *西北地质*, 35(4): 41–64
- 李亚萍, 孙桂华, 李锦轶, 王彦斌, 徐新, 何国琦, 贾金典. 2006. 吐哈盆地东缘泥盆纪花岗岩的确定及其地质意义. *地质通报*, 25(8): 932–936
- 李智明, 赵仁夫, 霍瑞平, 王庆明. 2006. 新疆土屋-延东铜矿田地质特征. *地质与勘探*, 42(6): 1–4
- 刘德权, 陈毓川, 王登红, 唐延龄, 周汝洪, 王金良, 李华芹, 陈富文. 2003. 土屋-延东铜钼矿田与成矿有关问题的讨论. *矿床地质*, 22(4): 324–344
- 刘敏, 朱弟成, 赵志丹, 王立全, 莫宣学, 周长勇. 2009. 西藏冈底斯东部然乌地区早白垩世岩浆混合作用: 锆石 SHRIMP U-Pb 年龄和 Hf 同位素证据. *地学前缘*, 16(2): 1446–1455
- 刘新秒. 2000. 后碰撞岩浆岩的大地构造环境及特征. 前寒武纪研究进展, 23(2): 121–127
- 姜峰, 喻亨祥. 2007. 新疆北部后碰撞构造环境特征初析. *中国科技*

- 信息, (22): 19-20
- 罗照华, 莫宣学, 卢欣祥, 陈必河, 柯珊, 侯增谦, 江万. 2007. 透岩浆流体成矿作用: 理论分析与野外证据. 地学前缘, 14(3): 165-183
- 罗照华, 卢欣祥, 陈必河, 黄凡, 杨宗锋, 王秉璋. 2008. 碰撞造山带斑岩型矿床的深部约束机制. 岩石学报, 24(3): 447-456
- 罗照华, 卢欣祥, 许俊玉, 刘翠, 李德东. 2010. 成矿侵入体的岩石学标志. 岩石学报, 26(8): 2247-2254
- 罗照华. 2012. 小岩体成大矿学说的内涵和意义. 西北地质, 45(4): 204-215
- 莫宣学, 董国臣, 赵志丹, 周肃, 王亮亮, 邱瑞照, 张风琴. 2005. 西藏冈底斯带花岗岩的时空分布特征及地壳生长演化信息. 高校地质学报, 11(3): 281-290
- 潘鸿迪, 申萍, 陈刚, 杨俊弢, 赵云江, 代华五. 2013. 新疆土屋斑岩铜矿床火山-侵入杂岩体、成矿岩石及其蚀变. 矿床地质, 32(4): 794-808
- 秦克章. 2000. 新疆北部中亚型造山带与成矿作用. 博士后出站报告. 北京: 中国科学院地质与地球物理研究所, 71-157
- 秦克章, 方同辉, 王书来, 朱宝清, 冯益民, 于海峰, 修群业. 2002. 东天山板块构造分区、演化与成矿地质背景研究. 新疆地质, 20(4): 302-308
- 芮宗瑶, 刘玉琳, 王龙生, 王义天. 2002. 新疆东天山斑岩型铜矿带及其大地构造格局. 地质学报, 76(1): 83-94
- 芮宗瑶, 张立生, 陈振宇, 王龙生, 刘玉琳, 王义天. 2004. 斑岩铜矿的源岩或源区探讨. 岩石学报, 20(2): 229-238
- 申萍, 潘鸿迪, 董连慧, 杨俊弢, 沈远超, 代华五, 关维娜, 赵云江. 2012. 新疆延东斑岩铜矿床火山机构、容矿岩石及热液蚀变. 岩石学报, 28(7): 1966-1980
- 唐俊华, 顾连兴, 张遵忠, 吴昌志, 三金柱, 汪传胜, 刘四海, 张光辉. 2007. 东天山咸水泉片麻状花岗岩特征、年龄及成因. 岩石学报, 23(8): 1803-1820
- 王福同, 冯京, 胡建卫, 王磊, 姜立丰, 张征. 2001. 新疆土屋大型斑岩铜矿床特征及发现意义. 中国地质, 28(1): 36-39
- 王京彬, 徐新. 2006. 新疆北部后碰撞构造演化与成矿. 地质学报, 80(1): 23-31
- 王京彬, 王玉往, 何志军. 2006. 东天山大地构造演化的成矿示踪. 中国地质, 33(3): 461-469
- 王龙生, 李华芹, 刘德权, 陈毓川. 2005. 新疆哈密维权银(铜)矿床地质特征和成矿时代. 矿床地质, 22(3): 280-284
- 王强, 赵振华, 许继峰, Wyman DA, 熊小林, 资峰, 白正华. 2006. 天山北部石炭纪埃达克岩-高镁安山岩-富Nb岛弧玄武岩: 对中亚造山带显生宙地壳增生与铜金成矿的意义. 岩石学报, 22(1): 11-30
- 王志良, 毛景文, 张作衡, 左国朝, 王龙生. 2006. 新疆天山斑岩铜矿地质特征、时空分布及其成矿地球动力学演化. 地质学报, 80(7): 943-955
- 吴昌志, 张遵忠, Khin Z, Fernando DP, 唐俊华, 郑远川, 汪传胜, 三金柱. 2006. 东天山觉罗塔格红云滩花岗岩年代学、地球化学及其构造意义. 岩石学报, 22(5): 1121-1134
- 吴兆宁, 黄建华, 玉素甫艾力, 戚冉, 木合塔尔·扎日, 杨向荣, 迪力夏提, 韩文清. 2007. 新疆土屋铜矿床某些成矿地球化学特征探讨. 新疆地质, 25(2): 160-163
- 熊小林, 蔡志勇, 牛贺才, 陈义兵, 王强, 赵振华, 吴金华. 2005. 东天山晚古生代埃达克岩成因及铜金成矿意义. 岩石学报, 21(3): 967-976
- 翟裕生, 王建平, 彭润民, 刘家军. 2009. 叠加成矿系统与多成因矿床研究. 地学前缘, 16(6): 282-290
- 翟裕生, 姚书振, 蔡克勤. 2011. 矿床学. 第三版. 北京: 地质出版社
- 张达玉, 周涛发, 袁峰, 范裕, 刘帅, 彭明兴. 2010. 新疆东天山地区延西铜矿床的地球化学、成矿年代学及其地质意义. 岩石学报, 26(11): 3327-3338
- 张连昌, 秦克章, 英基丰, 夏斌, 舒建生. 2004. 东天山土屋-延东斑岩铜矿带埃达克岩及其与成矿作用的关系. 岩石学报, 20(2): 259-268
- 赵泽南, 王银宏, 王建平, 董立帅, 张方方, 刘彬. 2014. 土屋铜矿企鵝山群火山岩地球化学特征及其地质意义. 矿物岩石, 34(1): 63-69
- 周涛发, 袁峰, 张达玉, 范裕, 刘帅, 彭明兴, 张建滇. 2010. 新疆东天山觉罗塔格地区花岗岩类年代学、构造背景及其成矿作用研究. 岩石学报, 26(2): 478-502
- 朱志敏, 熊小林, 初凤友, 吴云辉. 2013. 新疆东天山白山钼矿深部岩体地球化学特征及成因意义. 岩石学报, 29(1): 167-177